

See discussions, stats, and author profiles for this publication at: <https://www.researchgate.net/publication/231709265>

The Effect of Molecular Architecture on the Thermotropic Behavior of Poly[11- (4'-cyanophenyl-4'' -Phenoxy)undecyl Acrylate] and Its Relation to Polydispersity

ARTICLE in *MACROMOLECULES* · JANUARY 1998

Impact Factor: 5.8 · DOI: 10.1021/ma971279f

CITATIONS

109

READS

17

3 AUTHORS:



Andrea M Kasko

University of California, Los Angeles

32 PUBLICATIONS 1,248 CITATIONS

SEE PROFILE



Amy Heintz

Battelle Memorial Institute

12 PUBLICATIONS 428 CITATIONS

SEE PROFILE



Coleen Pugh

University of Akron

84 PUBLICATIONS 1,429 CITATIONS

SEE PROFILE

The Effect of Molecular Architecture on the Thermotropic Behavior of Poly[11-(4'-cyanophenyl-4''-phenoxy)undecyl acrylate] and Its Relation to Polydispersity

Andrea M. Kasko, Amy M. Heintz, and Coleen Pugh*

Department of Chemistry, Macromolecular Science and Engineering Center, University of Michigan, Ann Arbor, Michigan 48109-1055

Received August 25, 1997; Revised Manuscript Received November 10, 1997

ABSTRACT: Contrary to theoretical predictions on rodlike molecules (mixture of axial ratios) and previous experimental speculations on side chain liquid crystalline polymers (mixture of molecular weights), the breadth of the isotropization transition of poly[11-(4'-cyanophenyl-4''-phenoxy)undecyl acrylate] is not broadened by polydispersity in chain length alone. Instead, it is broadened by the limited miscibility of a mixture of branched structures. SCLCPs and their mesogenic side chains can therefore be treated as mixtures of random coils and monodisperse rods. This was demonstrated by comparing the thermotropic behavior of linear and three-arm star poly[11-(4'-cyanophenyl-4''-phenoxy)undecyl acrylate]s prepared by atom-transfer radical polymerization (ATRP), and their binary blends and unmixed composites. The biphasic region of linear polymers with $\text{pdi} = 1.15\text{--}1.49$, and of their binary mixtures, is extremely narrow. Although 3-arm star polymers with $\text{pdi} = 1.11\text{--}2.20$ also exhibit extremely narrow isotropization transitions, binary mixtures of the star polymers with significant differences in branching density have limited miscibility and broad isotropization transitions. The broad isotropization transition of unfractionated poly[11-(4'-cyanophenyl-4''-phenoxy)undecyl acrylate] prepared by standard radical polymerization indicates that it also contains a mixture of branched structures due to chain transfer to polymer at high monomer conversion. 11-(4'-Cyanophenyl-4''-phenoxy)undecyl acrylate is the most highly functionalized monomer to be polymerized by ATRP, and the resulting 3-arm star polymers are the first star polymers synthesized by ATRP.

Introduction

One of the most fundamental structure/property relationships of side chain liquid crystalline polymers (SCLCPs) that is still unknown is the effect of polydispersity. In some cases, the temperature and nature of the mesophase(s) depend not only on the degree of polymerization but also on the molecular weight distribution.^{1,2} For example, the sc mesophase of polydisperse poly[6-(4'-cyanophenyl-4''-phenoxy)hexyl vinyl ether] ($\text{pdi} = 1.9$) was not detected by differential scanning calorimetry (DSC), although it was readily apparent in samples with narrower polydispersity ($\text{pdi} = 1.2$).² However, broad polydispersity is generally believed to cause broad phase transitions. In contrast to low-molar-mass liquid crystals (LMMLCs), which undergo phase transitions over a few degrees, SCLCPs often exhibit extremely broad transitions. This wide biphasic region, in which two phases such as a mesophase and the isotropic melt coexist, is evidently due to the fact that polymers are polydisperse. For example, fractionated samples of poly[11-(4'-cyanophenyl-4''-phenoxy)undecyl acrylate] undergo isotropization over a narrower temperature range than the original polymer prepared by free-radical polymerization.³ In contrast, the transitions of most well-defined SCLCPs prepared by controlled ("living") polymerizations are relatively narrow.⁴ The effect of polydispersity was therefore investigated by blending well-defined ($\text{pdi} < 1.28$) poly[5-[[n -(4'-(4''-methoxyphenyl)phenoxy)alkyl]carbonyl]bicyclo[2.2.1]hept-2-ene]s of varying molecular weights ($\text{DP}_n = 5\text{--}145$) to create polydisperse samples ($\text{pdi} = 2.50\text{--}4.78$).⁵ In this case, both monodisperse samples

and multimodal blends underwent the nematic–isotropic transition over a narrow temperature range. Polydispersity also had no effect on the transition temperatures, which were determined simply by the number-average degree of polymerization.

Since polydispersity created by blending linear polymers has no effect on the thermotropic behavior of polynorbornenes,⁵ whereas fractionation of polyacrylates prepared by radical polymerizations results in narrower biphasic regions,³ we must consider the potential sources of polydispersity. Mesogenic monomers are highly functionalized with a number of sites capable of chain transfer in free-radical polymerizations. Chain transfer to polymer should result in chain branching and broad polydispersity at high monomer conversion. Therefore, the broad phase transitions of SCLCPs may be caused by the immiscibility of a mixture of molecular architectures caused by chain branching at the end of free-radical polymerizations.

Similarly, the melting behavior of polyethylene and other crystalline polymers is strongly affected by molecular architecture. For example, high-density polyethylene (HDPE) is quite linear (0.05–0.3 branch/50 repeat units)⁶ and therefore highly crystalline (70–90%),⁷ with a high melting temperature ($T_m = 130\text{--}135\text{ }^\circ\text{C}$).⁸ However, its polydispersity is high ($\text{pdi} = 5\text{--}10$) due to the multiple initiation sites in the Ziegler–Natta polymerizations used to produce it.⁷ Low density polyethylene (LDPE) is also polydisperse ($\text{pdi} = 3\text{--}20$), but the broad polydispersity is caused by chain transfer to polymer during radical polymerization.⁷ LDPE is therefore highly branched (1.5–3.0 branches/50 repeat units) and less crystalline (40–60%) than linear polyethylene,⁷ with a significantly lower melting tempera-

* To whom correspondence should be addressed.

ture ($T_m = 108\text{--}115\text{ }^\circ\text{C}$).⁹ In contrast to LDPE, which has both short- and long-chain branches, the branch lengths of linear low-density polyethylenes (LLDPE) are more controlled since they are synthesized by Ziegler–Natta or metallocene-initiated copolymerizations of ethylene with an α -olefin such as butene, hexene or octene.⁷ The melting temperatures of LLDPEs are intermediate between those of HDPE and LDPE. In general, the melting temperature,^{10,11} enthalpy of fusion,^{10,12} degree of crystallinity,^{11–15} and rate of crystallization^{14,16} of polyethylene decrease as the extent of short-chain branching increases.

Crystalline polymers such as linear polyethylene can be fractionated into high- and low-molecular-weight components by isothermal crystallization in the biphasic region after cooling from the homogeneous melt.⁹ Similarly, both main-chain¹⁷ and side chain¹⁸ liquid crystalline homopolymers can be fractionated by isothermal ordering in the biphasic region for several hours. Both experimentalists^{17–19} and theoreticians^{20–22} conclude that the biphasic region of liquid crystalline homopolymers is due to selective partitioning of different chain lengths between anisotropic and isotropic domains (or two different anisotropic domains) and that the breadth of the transition reflects the molecular weight distribution of the sample. Although some of the theories take partial flexibility into account,²² they are based on a distribution of rod lengths,²³ which should not vary as a function of molecular weight when the mesogen (rod) is attached as a side chain to the polymer backbone.^{24–26} In addition, the broad transitions observed by DSC are observed under dynamic conditions, not isothermal conditions that force phase segregation of individual chains with different transition temperatures. Under dynamic conditions, if the individual chains are miscible in both phases coexisting at the transition, the polymer sample should exhibit a single transition representing an average of those chains.

This is consistent with the thermal behavior of crystalline linear polymers, in which the breadth and shape of a single DSC endotherm represents the distribution of lamellar thicknesses and their melting temperatures,²⁷ not the distribution of chain lengths. That is, unless polydisperse blends of linear polyethylene are crystallized isothermally in the biphasic region, they form homogeneous solid mixtures with a single melting transition and uniform morphology.²⁸ In contrast, blends of linear and branched polyethylene of various branched polyethylenes tend to phase segregate,^{9,29,30} with the immiscibility increasing as the branch content of the two components becomes more dissimilar.^{10,15,31–33} In addition, although the *melts* of HDPE/LDPE^{30,34} blends and HDPE/LLDPE^{15,32,33} with lower branch contents (<4 branches/50 repeat units when $M_w \leq 10^5$) are homogenous, those of HDPE/LLDPE³² with high branch contents (>8 branches/50 repeat units, $M_w \sim 10^5$) are heterogeneous. Even pure LLDPE is compositionally heterogeneous,^{12,35} with ~ 0.2 vol % that is much more highly branched and immiscible in both the solid state and melt.³⁵

Most SCLCPs are still prepared by free-radical polymerizations. Although termination by radical–radical coupling and disproportionation occur at diffusion-controlled rates and are therefore unavoidable in radical polymerizations,⁷ controlled radical polymerizations of styrene,^{36–40} acrylates,^{39,40} and methacrylates⁴¹ were recently developed. These “living” polymerizations

minimize termination by maintaining a low concentration of propagating radicals in dynamic equilibrium with a high concentration of dormant covalent chains. However, chain transfer to monomer and/or polymer is not affected since both propagation ($R_p = k_p[M^\bullet][M]$) and chain transfer ($R_{trX} = k_{trX}[M^\bullet][X]$) are first order in propagating radicals. Nevertheless, chain transfer will not be detected if $k_p/k_{tr} \geq 10[M]_0/[I]_0 \sim 10DP_n$.⁴²

We can therefore prepare monodisperse SCLCPs corresponding to those synthesized previously by conventional radical polymerizations, but with controlled degrees of polymerization and well-defined molecular architectures. Since the fractionation study of poly[11-(4'-cyanophenyl-4''-phenoxy)undecyl acrylate] provided the most direct evidence that its smectic A–isotropic (s_A –i) biphasic region narrows as the polydispersity decreases,³ we have prepared a series of linear and 3-arm star poly[11-(4'-cyanophenyl-4''-phenoxy)undecyl acrylate]s by atom transfer radical polymerization (ATRP³⁸). As a first step in determining whether the broad phase transitions of the corresponding polymer prepared by conventional radical polymerization is due to polydispersity in molecular architecture, and/or to polydispersity in chain length, this paper compares its thermotropic behavior to that of the linear and star homopolymers, as well as to their binary blends.

Results and Discussion

Conventional Radical Polymerization. Although the fractionation study of poly[11-(4'-cyanophenyl-4''-phenoxy)undecyl acrylate] clearly demonstrated that the fractionated polymers undergo isotropization over a narrower temperature range than the original polymer isolated from the conventional free-radical polymerization,³ only the intrinsic viscosities of the polymers were reported, with no information on their polydispersities. We have therefore duplicated these experiments as much as possible, given the limited experimental details.^{3,43} Using 1 wt % AIBN relative to monomer in THF at 60 $^\circ\text{C}$, the conventional radical polymerization of 11-(4'-cyanophenyl-4''-phenoxy)undecyl acrylate went to $\sim 83\%$ conversion. After carefully removing monomer and recovering oligomeric material, we isolated polymer with $M_n = 2.52 \times 10^4$ and $pdi = 3.43$ in 72% yield. This polymer was then fractionated into seven samples by fractional precipitation from THF using methanol. As summarized in Table 1, all of the fractions have narrower polydispersities ($pdi = 1.57\text{--}2.04$) than the original sample, and their molecular weights vary from 5.79×10^3 to 4.31×10^4 .

The isotropization region of the DSC scans of these seven fractions and the original polymer are plotted in Figure 1. In contrast to the isotropization transition of the unfractionated literature polymer, which has a low-temperature tail,³ the isotropization transition of the unfractionated polymer shown in Figure 1 is symmetric. Nevertheless, the polymers from this study correspond well to the unfractionated and fractionated poly[11-(4'-cyanophenyl-4''-phenoxy)undecyl acrylate]s prepared previously. For example, both the unfractionated polymer from this study and that from the literature³ undergo the s_A –i transition over $\sim 35\text{ }^\circ\text{C}$. However, this measurement is somewhat subjective, and we therefore prefer to represent the breadth of the transitions as the full width at half of the maximum peak intensity (fwhm). The full width at half-maximum of the unfractionated polymer from this study is 17.0 $^\circ\text{C}$; that

Table 1. Fractionation of Poly[11-(4'-cyanophenyl-4''-phenoxy)undecyl acrylate] Prepared by Conventional Radical Polymerization.

fraction	% of original polymer	% of fractionated polymer	$M_n \times 10^{-3}$	GPC ^a		isotropization (°C)	
				\overline{DP}_n	pdi	T_i	fwhm
original	100		25.2	60	3.43	140	17.0
1	22	26	43.1	103	1.57	150	6.25
2	5	6	29.5	70	1.75	144	8.93
3	14	17	24.0	57	1.96	145	7.14
4	22	27	20.9	50	1.74	142	8.48
5	4	5	12.0	29	2.04	133	7.77
6	10	12	8.63	21	1.78	125	10.7
7	6	7	5.79	14	1.89	106	10.2
reblend	69 ^b	83 ^b	23.4	56	3.75	136	16.5

^a Number-average molecular weight (M_n) and polydispersity ($pdi = M_w/M_n$) determined by gel permeation chromatography (GPC) relative to polystyrene using a UV detector; number-average degree of polymerization (\overline{DP}_n) calculated by dividing M_n by 419.56 and not taking end groups into account. ^b If 100% of each fraction had been reblended.

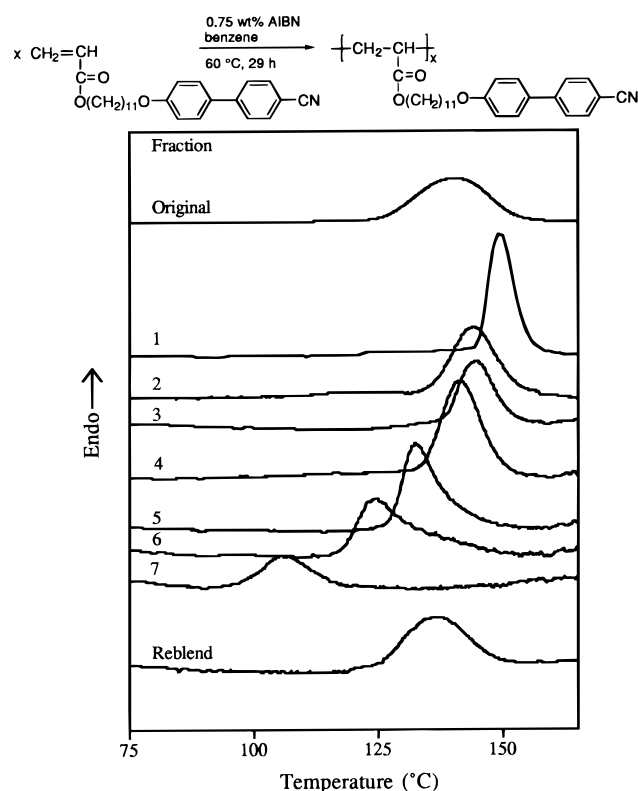


Figure 1. Normalized differential scanning calorimetry traces (10 °C/min) of poly[11-(4'-cyanophenyl-4''-phenoxy)undecyl acrylate] prepared by conventional radical polymerization, of samples of decreasing molecular weight fractionated from it by adding methanol to its THF solution, and of the reblended fractions.

from the literature³ is 18.4 °C. As shown in Figure 1 and summarized in Table 1, the isotropization transitions of all of the fractions are significantly narrower (fwhm = 6.25–10.7 °C) than that of the original polymer. Similarly, the samples fractionated with ethanol from a 1,2-dichloroethane solution of the literature polymer underwent isotropization over 15–25 °C (fwhm = 6.3–8.6 °C).³ However, both the lower molecular weight samples from this study and those from the literature³ have broader transitions than the higher molecular weight samples. Although the end groups are relatively small and are chemically bonded to the polymers, this indicates that the end groups have limited miscibility with the mesogenic side chains. Since end groups have a greater influence as the molecular weight decreases, they evidently broaden the breadth of the phase transitions of lower molecular

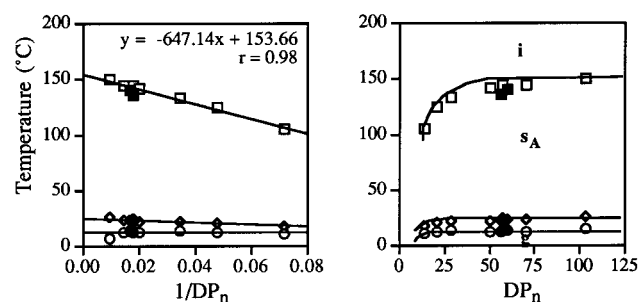


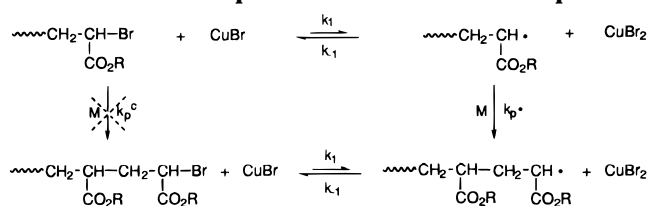
Figure 2. Dependence of the glass (●, ○), smectic C–smectic A (◆, ◇), and smectic A–isotropic (■, □) phase transition temperatures of unfractionated (and reblended) poly[11-(4'-cyanophenyl-4''-phenoxy)undecyl acrylate] prepared by classic radical polymerization (●, ◆, ■), and samples fractionated from it (○, ◇, □), as a function of the number-average degree of polymerization and the inverse number-average degree of polymerization. Infinite molecular weight transitions: T_g 12 °C, T_{SC-SA} 26 °C, T_{SA-I} 154 °C.

weight polymers. Any immiscibility between the polymer backbone and the mesogenic side chains will not influence the molecular weight dependence of the breadth of the phase transitions as suggested previously,⁴⁴ since the backbone and side chains are the same regardless of molecular weight.

The glass and s_A – i transition temperatures are plotted in Figure 2 as a function of the number-average degree of polymerization (\overline{DP}_n) and \overline{DP}_n^{-1} ; these polymers also exhibit a s_C – s_A transition at a temperature immediately above the glass transition temperature. However, the proximity of the s_C – s_A and glass transitions hinders the s_C mesophase from reaching thermodynamic equilibrium with repeated heating and cooling cycles, and we therefore did not examine it further. The isotropization temperature of the unfractionated polymer ($M_n = 2.52 \times 10^4$) is 140 °C, whereas those of the fractionated polymers vary from 106 to 150 °C with increasing molecular weight. The isotropization temperature of the original polymer from the literature was 144 °C,³ which indicates that its molecular weight was slightly higher than the polymer we prepared. The isotropization temperature of the five fractionated literature polymers varied from 113 to 147 °C with increasing intrinsic viscosity. As shown in Figure 2, the transition temperatures of the fractionated polymers prepared by conventional radical polymerization reach a constant value at ~ 50 repeat units. This corresponds to $T_i = 154$ °C for an infinite molecular weight poly[11-(4'-cyanophenyl-4''-phenoxy)undecyl acrylate] according to the extrapolation to $\overline{DP}_n^{-1} = 0$.

Synthesis of Linear and Three-Arm Star Polymers by ATRP. As reported in the previous section, the conventional radical polymerization of 11-[(4'-cyanophenyl-4''-phenoxy)undecyl] acrylate using AIBN as the initiator in THF at 60 °C produced a polymer with $\text{pdi} = 3.43$. This polydispersity is wider than expected for a radical polymerization with termination by coupling ($\text{pdi} = 1.5$) or disproportionation ($\text{pdi} = 2.0$) and, therefore, indicates that the polydispersity is broadened by either autoacceleration or chain transfer to monomer and/or polymer at high monomer conversion. Autoacceleration is less important at higher temperatures. Chain transfer to polymer (and monomer) produces branched structures, which have different solubilities, transition temperatures, and enthalpies of transitions than the corresponding linear polymers. Since we cannot readily identify the extent of branching in either the original polymer or its fractions, we have begun synthesizing and characterizing linear and star poly-[11-(4'-cyanophenyl-4''-phenoxy)undecyl acrylate]s with controlled branching by atom transfer radical polymerization. For example, 3-arm star polymers correspond to a linear polymer with one branch point along the polymer backbone. This is the first example of a star polymer prepared by ATRP.

Scheme 1. Accepted Mechanism of Atom Transfer Radical Polymerizations Using Alkyl Bromide-Initiated Polymerizations of Acrylates in the Presence of Cuprous Bromide as an Example.



Scheme 2. Synthesis of Poly[11-(4'-cyanophenyl-4''-phenoxy)undecyl acrylate]s with Linear and Three-Arm Star Architectures by ATRP

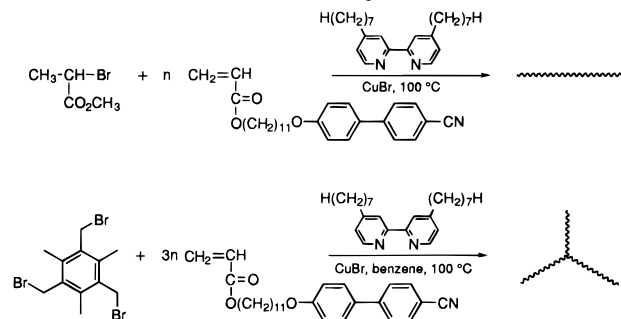


Table 2 summarizes the results of the atom transfer radical polymerizations of 11-(4'-cyanophenyl-4''-phenoxy)undecyl acrylate using $[M]_0/[I]_0 < 300$. Linear polymers with 8–70 repeat units were produced by bulk polymerizations using methyl 2-bromopropionate as the initiator. In this case, the chemical structure and, therefore, the reactivity of the initiator and propagating polymer are nearly identical, and the resulting polymers have relatively narrow, monomodal molecular weight distributions ($\text{pdi} = 1.15\text{--}1.49$). In contrast, the trifunctional initiator is based on benzyl bromide initiating sites, which are also relatively efficient at initiating acrylates.³⁹ Although a small amount of benzene was added to the 2,4,6-tris(bromomethyl)mesitylene-initiated polymerizations to reduce their viscosity and enable stirring, it was difficult to attain complete conversion at high monomer to initiator ratios; it was also difficult to attain complete conversion of the linear polymers when $[M]_0/[I]_0 > 60$. The highest molecular weight 3-arm star polymer containing 90 repeat units was therefore synthesized using a much higher ratio of monomer to initiator. The final 3-arm star polymers used in this study contain 20–90 repeat units. Their molecular weight distributions are narrow when $\text{DP}_n < 60$ ($\text{pdi} = 1.15\text{--}1.24$), whereas the two highest molecular weight polymers have rather broad polydis-

Table 2. Synthesis of Poly[11-(4'-cyanophenyl-4''-phenoxy)undecyl acrylate] by Atom Transfer Radical Polymerizations^a

[M] ₀ /[I] ₀	theor ^b	time	yield ^c	GPC ^d		
	$M_n \times 10^{-3}$	(h)	(%)	$M_n \times 10^{-3}$	DP _n	pdi
linear						
5	2.26	0.7	70	3.68	8	1.15
10	4.36	1.2	70	5.05	12	1.16
10	4.36	3	52	7.83	18	1.33
20	8.56	46	45	10.0	24	1.21
30	12.8	7	69	16.8	40	1.30
40	16.9	20	62	15.4	36	1.34
50	21.1	16	84	29.4	70	1.49
three-arm star						
15	6.69	3	67	8.68	20	1.15
31	13.4	20	85	12.5	29	1.24
61	26.0	37	48	21.1	49	1.22
61	26.0	24	68	25.7	61	1.79
87	36.9	36	46	23.5	55	1.25
99	41.9	96	46	18.1	42	1.11
139	58.7	84	22	20.3	47	1.18
273	115	132	66	38.2	90	2.20

^a Using 1:3:1 CuBr/4,4'-diheptyl-2,2'-dipyridyl/initiating site at 100 °C; bulk polymerizations of linear polymers; 3-arm star polymers in a minimum amount of benzene. ^b Assuming 100% conversion and taking end groups into account: linear $M_n = 167.01 + (419.56[M]_0/[I]_0)$; 3-arm star $M_n = 398.98 + (419.56[M]_0/[I]_0)$. ^c After copper and monomer completely removed by multiple reprecipitations. ^d Number-average molecular weight (M_n), number-average degree of polymerization (DP_n), and polydispersity (pdi = M_w/M_n) determined by gel permeation chromatography (GPC) relative to polystyrene using mean of RI and UV detectors.

persities of 1.79–2.20. The molecular weight distribution of the 3-arm star polymer with DP_n = 90 is monomodal and that with DP_n = 61 is bimodal.

Effect of Copper on the Thermal Stability of Polymers Prepared by ATRP. As outlined in Scheme 1, Cu(I) (complexed with bipyridine) homolytically cleaves the carbon–halogen bond of the initiating and polymeric alkyl halides to generate a radical and Cu(II). This occurs at 80–100 °C with alkyl bromides.^{38–40} The final polymers have the same alkyl bromide chain ends as the initiator and the dormant propagating chains. Therefore, residual copper and/or the bromide chain ends may lower the thermal stability of polymers prepared by ATRP, which will result in decomposition or cross-linking, as well as changes in the molecular weight distribution.

Aqueous and methanolic solutions of ammonium chloride remove copper salts from organic compounds. For example, polymers generated by ATRP eventually become colorless when they are repeatedly precipitated in methanolic ammonium chloride, whereas the ammonium chloride filtrate becomes blue when it extracts copper salts. Figure 3 shows the thermogravimetric analyses (TGA) of linear poly[11-(4'-cyanophenyl-4''-phenoxy)undecyl acrylate] (DP_n = 10, pdi = 1.17) prepared by ATRP as a function of the number of reprecipitations in methanolic ammonium chloride, following the initial precipitation in methanol. Most of the copper salts are still present in the polymer after the first precipitation in methanol. The data in Table 3 demonstrate that residual copper significantly decreases the decomposition onset temperature of the polymer. The decomposition temperature first jumps from 295 to 302 °C after the initial precipitation in methanolic ammonium chloride (precipitation 2) and then increases relatively steadily (304–319 °C) with subsequent reprecipitations. There is no change in the

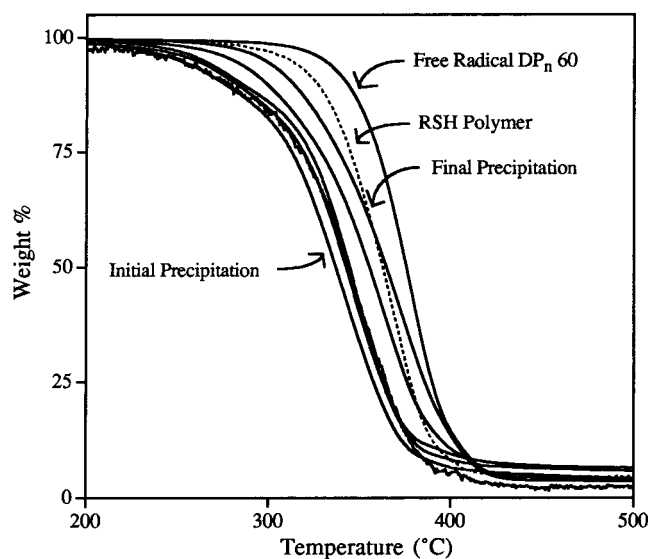


Figure 3. Effect of residual copper on the thermogravimetric analyses (10 °C/min under air) of linear poly[11-(4'-cyanophenyl-4''-phenoxy)undecyl acrylate] (DP_n = 10, pdi = 1.17) prepared by ATRP as a function of the number of (re)precipitations (increasing stability) in cold saturated aqueous NH₄Cl/methanol (3:9). The TGA scans of the corresponding polymers (DP_n = 60, pdi = 3.43; DP_n = 11, pdi = 1.20) prepared by conventional radical polymerization are shown for comparison.

molecular weight or polydispersity of the polymer from the first to the last precipitation (DP_n = 10, pdi = 1.17).

However, the decomposition onset temperature is an extrapolated value. Figure 3 demonstrates that the decomposition begins gradually at a lower temperature in the presence of copper. In contrast, decomposition is much more abrupt and at a higher temperature in the samples that have been reprecipitated several times in methanolic ammonium chloride to remove copper. The TGA scan of the corresponding polymer (DP_n = 60, pdi = 3.43) prepared by conventional radical polymerization is also shown in Figure 3. It decomposes abruptly at 346 °C and is therefore significantly more stable than the low-molecular-weight polymer prepared by ATRP, even when all of the copper has been removed. Since this may be due simply to differences in molecular weight, we prepared a polymer with the same molecular weight as the ATRP (DP_n = 10, pdi = 1.17) sample by standard radical polymerization in the presence of 1-decanethiol as a chain-transfer agent (DP_n = 11, pdi = 1.20). The structure of this polymer and its end groups are compared to those of the linear polymers prepared by ATRP in Chart 1. Although typical C–S and C–Br bond energies are identical (276 kJ/mol),⁴⁶ the polymer prepared by conventional radical polymerization is 11 °C more stable than the polymer prepared by ATRP. This is evidently because the C–S bond at a primary carbon is more stable than the C–Br bond at a secondary carbon bonded to carbonyl. However, all of the polymers prepared by ATRP and by conventional radical polymerizations decompose in one step with the same weight loss (96%).

The thermal stability of the polymer may possibly be used to help confirm the extent of bimolecular coupling in atom transfer radical polymerizations. As shown in Chart 1, polymers that terminate by bimolecular coupling do not have alkyl bromide chain ends. Comparison of the monomer to initiator ratios and GPC-determined number-average degrees of polymerization

Table 3. Thermal Behavior of Poly[11-(4'-cyanophenyl-4''-phenoxy)undecyl acrylate] Prepared by ATRP as a Function of Residual Copper

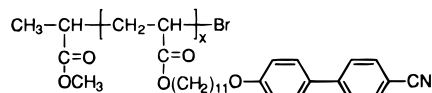
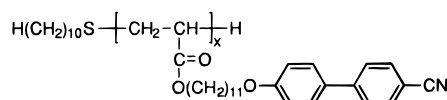
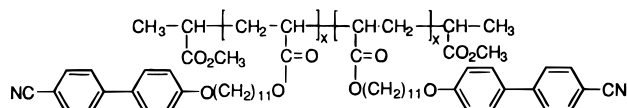
polymer sample	TGA		isotropization (°C)	
	onset (°C) of dec	% wt loss	T_i	fwhm
ATRP				
precip 1 ($DP_n = 10$, ^a $pdi = 1.17$)	295	96.8	95	7.50
precip 2	302	97.3	96	6.15
precip 3	304	96.0	96	6.50
precip 4	301	95.8	95	6.50
precip 5	309	94.6	95	7.50
precip 6 ($DP_n = 10$, ^a $pdi = 1.17$)	319	96.6	93	7.40
radical $DP_n = 60$, ^b $pdi = 3.43$	346	95.9	140	17.0
radical + RSH $DP_n = 11$, ^a $pdi = 1.20$	330	95.4	92	8.62

^a Takes end groups into account. ^b Does not consider end groups.

Table 4. Thermotropic Behavior of Poly[11-(4'-cyanophenyl-4''-phenoxy)undecyl acrylate] Prepared by ATRP^a

DP_n	GPC		TGA		transition temp (°C)			peak width (°C)		
	$M_n \times 10^{-3}$	pdi	onset (°C) of dec	% wt loss	$g-S_C$	S_C-S_A	S_A-i	DSC	fwhm	POM
linear										
8	3.68	1.15	322	93.5	7	12	97	24	6.70	22.7
12	5.05	1.16	308	99.7	8	14	107	28	7.59	19.2
18	7.83	1.33	318	97.3	12	20	122	36	8.21	16.4
24	10.0	1.21	330	96.1	14	22	126	24	5.36	15.1
36	15.4	1.34	328	95.1	14	23	134	25	5.36	12.7
40	16.8	1.30	328	97.1	12	21	133	19	5.36	11.8
70	29.4	1.49	337	97.2	17	26	141	18	4.46	8.7
three-arm star										
20	8.68	1.15	309	95.9	14	21	113	35	8.04	14.4
29	12.5	1.24	329	94.7	15	24	123	19	7.14	12.7
42	18.1	1.11	338	96.3	13	22	129	27	6.25	15.2
47	20.3	1.18	330	96.8	16	25	131	27	7.14	20.2
49	21.1	1.22	336	96.7	12	21	132	21	8.96	18.2
55	23.5	1.25	331	95.5	16	26	135	30	5.36	12.6
61	25.7	1.79	329	94.6	15	25	133	28	7.14	13.1
90	38.2	2.20	329	95.4	17	27	139	23	4.46	13.0

^a From DSC on heating at 10 °C/min; peak width determined by DSC on heating from the deviation from the baseline of the endotherm (DSC) and from the full width at half-maximum of the peak (fwhm), and by polarized optical microscopy (POM) on cooling at -10 °C/min from the mean of three measurements.

Chart 1. Comparison of the Chemical Structures of Linear Poly[11-(4'-cyanophenyl-4''-phenoxy)undecyl acrylate] Prepared by ATRP and by Standard Radical Polymerization in the Presence of 1-Decanethiol as a Chain-Transfer Agent.**ATRP****Free Radical****ATRP with bimolecular coupling**

in Table 2 of the linear polymers prepared by ATRP, and their thermal stability in Table 4, indicate that a few of the polymers have terminated primarily by bimolecular coupling. For example, the molecular weight of the linear polymer synthesized with $[M]_0/[I]_0 = 50$ is higher than expected ($DP_n = 70$, $pdi = 1.49$), and its decomposition onset temperature (337 °C) is much higher than the rest of the polymers (318–330

°C); its molecular weight distribution is monomodal. The decomposition onset temperature (308 °C) of the linear polymer with $DP_n = 12$ ($pdi = 1.16$) is lower than that of the rest of the polymers, indicating that it is contaminated with residual copper. The decomposition onset temperatures of the 3-arm star polymers are much less variable. With the exception of the polymer with $DP_n = 20$ (309 °C), the 3-arm star polymers decompose at ~330 °C. The decomposition temperatures of the two star polymers with $DP_n = 42$ ($pdi = 1.11$) and $DP_n = 49$ ($pdi = 1.22$) are high, although their polymerizations did not go to completion. The molecular weight distribution of the $DP_n = 42$ polymer is monomodal, whereas that of the $DP_n = 49$ has a higher molecular weight shoulder. Although the molecular weight distribution of the 3-arm star polymer with $DP_n = 61$ is bimodal and symmetric, and evidently has a significant amount of chains that were terminated by bimolecular coupling, its decomposition onset temperature is normal. All of the linear and 3-arm star polymers prepared by ATRP decompose in one step with 93.5–99.7% weight loss.

Residual copper has essentially no effect on the breadth of the phase transitions. As shown in Figure 4 and summarized in Table 3, the isotropization transition of the polymer precipitated only in methanol is as narrow ($fwhm = 7.50$ °C) as those of the polymers subsequently precipitated in methanolic ammonium chloride ($fwhm = 6.15$ – 7.50 °C). However, we have found that residual copper is detrimental to both the breadth of the isotropization transition (260 °C) and the decomposition temperature of poly(biphenyl acrylate).⁴⁷

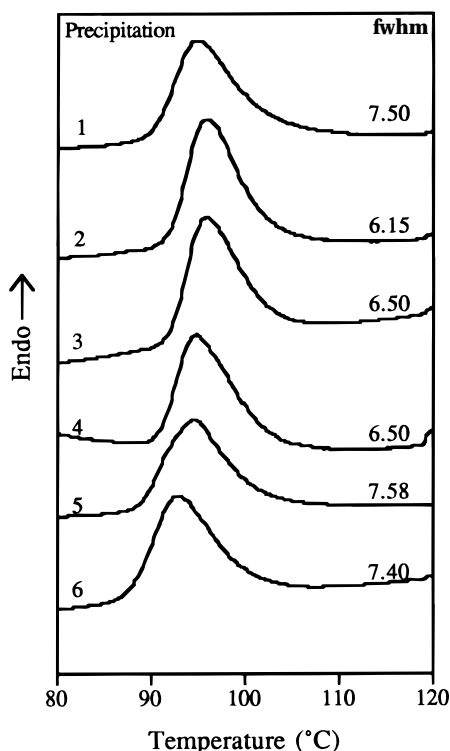


Figure 4. Effect of residual copper on the normalized differential scanning calorimetry traces (10 °C/min) of linear poly[11-(4'-cyanophenyl-4''-phenoxy)undecyl acrylate] ($DP_n = 10$, $pdi = 1.17$) prepared by ATRP as a function of the number of (re)precipitations in cold saturated aqueous NH_4Cl /methanol (3:9).

Therefore, ATRP is most useful for synthesizing SCLCPs with lower transition temperatures, although residual copper must be stringently removed to prevent decomposition and possibly anomalous thermotropic behavior.

Thermotropic Behavior of Linear and Three-Arm Star Polymers Prepared by ATRP. All of the poly[11-(4'-cyanophenyl-4''-phenoxy)undecyl acrylate]s prepared by ATRP were carefully purified to remove both residual copper and any unreacted monomer. Excess monomer was removed from polymerizations that did not go to full conversion by reprecipitating them from THF into a warm solution of ethanol and toluene (5:1), followed by slowly cooling to -78 °C before collecting the polymer. Figure 5 presents the normalized DSC heating scans of the linear polymers with degrees of polymerization of 8–70, and Figure 6 presents the normalized DSC heating scans of the 3-arm star polymers ($DP_n = 20$ –90). The s_C – s_A transitions are barely detectable because the polymers were not annealed for sufficient time after heating through isotropization; the s_A – i transition is not affected by annealing. As shown by the representative polarized optical micrographs in Figure 7, both the linear and 3-arm star polymers exhibit typical focal-conic fan textures after annealing for only a short time in the s_A mesophase.

As shown in Figures 5 and 6 and summarized in Table 4, the temperature of the glass and isotropization transitions increase as the molecular weight of both polymer series increases. However, the isotropization temperatures of the 3-arm star polymers are slightly lower than those of the linear polymers with similar molecular weights, which confirms that their molecular architectures are different. For example, the linear

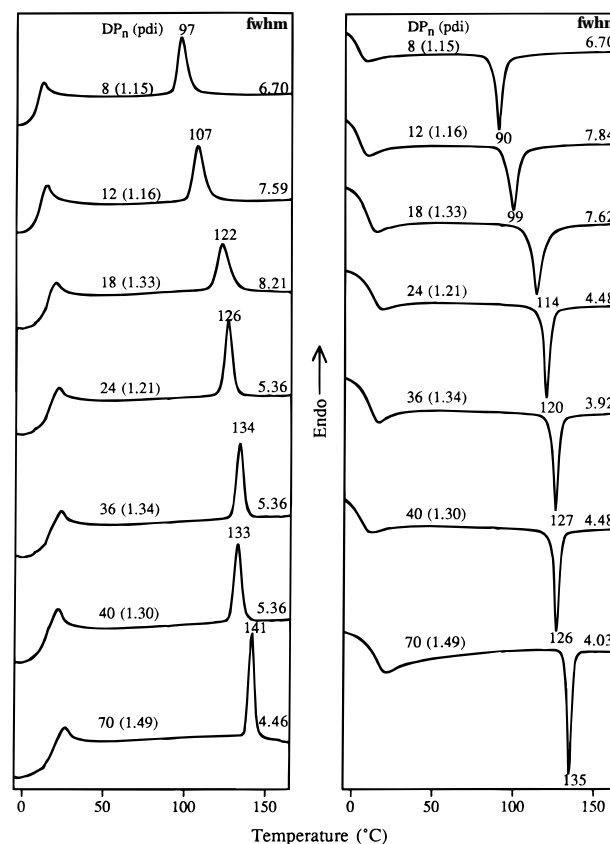


Figure 5. Normalized differential scanning calorimetry traces (10 °C/min) of linear poly[11-(4'-cyanophenyl-4''-phenoxy)undecyl acrylate]s prepared ATRP.

polymer with $DP_n = 40$ undergoes isotropization at 133 °C, whereas the 3-arm star polymer with $DP_n = 42$ undergoes isotropization at 129 °C. This lower temperature also does not correspond to the isotropization temperature of a single arm, since the corresponding linear polymer with $DP_n = 12$ undergoes isotropization at 107 °C. The isotropization transition of the linear polymers also levels off at a slightly lower degree of polymerization ($DP_n \approx 40$) than that of the 3-arm star polymers ($DP_n \approx 50$) (Figure 8), which again indicates that their molecular architectures are different. Nevertheless, both series extrapolate to exactly the same isotropization temperature (145 °C) at infinite molecular weight. This demonstrates that the effect of one branch point is insignificant at infinite molecular weight and that GPC is a reasonable method for comparing the molecular weight of these linear and 3-arm star SCLCPs. The glass and s_C – s_A transitions, especially of the 3-arm star polymers, are much less sensitive to increasing molecular weight.

The extrapolated isotropization temperature of the ATRP polymers (145 °C) is significantly lower than that of the fractionated polymers prepared by standard free-radical polymerization (154 °C). This is obviously not due to differences in end groups since end groups have no effect at infinite molecular weight. The primary difference between the polymers prepared by ATRP and those prepared by standard radical polymerization is presumably that some of the fractionated polymers are branched. Due to differences in solubility, fractional precipitation separates polymers according to differences in both molecular weight and molecular architecture. Therefore, the molecular architecture of the fractionated polymers from the standard radical polym-

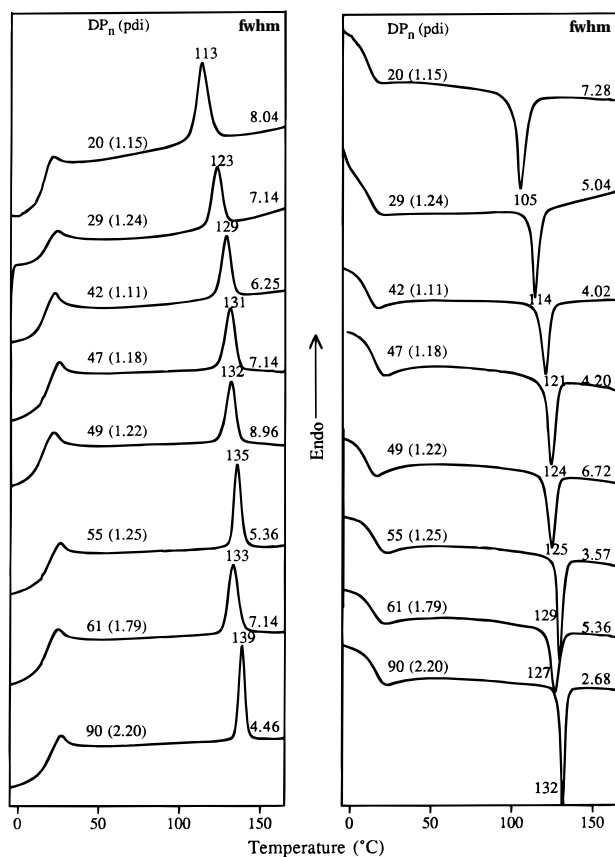


Figure 6. Normalized differential scanning calorimetry traces (10 °C/min) of 3-arm star poly[11-(4'-cyanophenyl-4''-phenoxy)undecyl acrylate]s prepared ATRP.

erization may be changing throughout the extrapolation in Figure 2, whereas the extrapolations in Figure 8 are based on a uniform molecular architecture. The glass (12–16 °C) and s_C – s_A (26 °C) transitions of all of the polymers extrapolate to the same values at infinite molecular weight.

Table 4 also lists the breadth of the isotropization transitions, determined by three different methods, of the linear and 3-arm star polymers prepared by ATRP. Although the deflection of the endotherm (or exotherm) from the baseline of the DSC scans represents the actual breadth of the transition, it is sensitive to baseline curvature. For example, Figure 6 shows that the isotropization endotherm of the 3-arm star polymer with DP_n = 55 is quite narrow. However, the breadth of the transition determined from the baseline of the DSC scan indicates that it is broader than those of most of the other samples. The biphasic temperature range can also be determined directly by polarized optical microscopy, although this can be highly subjective. In contrast, the full width at half-maximum is directly related to the breadth of the isotropization transitions in Figures 5 and 6 and is quite reproducible. We have therefore used the full width at half-maximum to describe the breadth of the phase transitions throughout the rest of this paper.

As shown in Figure 5 and summarized in Table 4, the isotropization transitions of the linear polymers are narrow in all cases (fwhm = 4.46–8.21 °C), and tend to be slightly narrower than even the fractionated samples from the conventional radical polymerization (Table 1). Similarly, the isotropization transitions of the 3-arm star polymers (Figure 6) are narrow, with fwhm = 4.46–

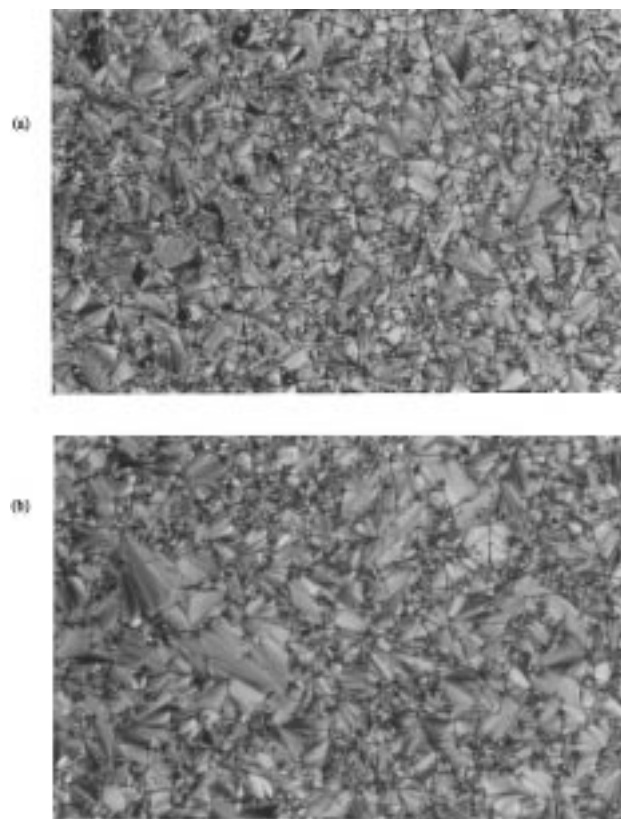


Figure 7. Polarized optical micrographs (200 \times) of the s_A focal-conic fan textures observed after annealing for 30 min upon cooling poly[11-(4'-cyanophenyl-4''-phenoxy)undecyl acrylate] from the isotropic melt: (a) 130.3 °C, linear polymer (DP_n = 40, pdi = 1.30); (b) 123.9 °C, 3-arm star polymer (DP_n = 42, pdi = 1.11).

8.96 °C. The highest molecular weight linear and 3-arm star polymers again have the narrowest transitions (fwhm = 4.46 °C). However, the highest molecular weight polymers from both the linear (DP_n = 70, pdi = 1.49) and 3-arm star (DP_n = 90, pdi = 2.20) series have the broadest polydispersities. This demonstrates that a broad monomodal, Gaussian-like distribution of chain lengths of a single architecture is not sufficient to broaden the breadth of the s_A – i transition of poly[11-(4'-cyanophenyl-4''-phenoxy)undecyl acrylate].

The most obvious component of a SCLCP that could result in a non-Gaussian-like distribution of molecular weights is monomer. We found that it was difficult to achieve complete monomer conversion in both the AIBN-initiated and ATRP polymerizations at higher monomer to initiator ratios. In addition, since both NMR and GPC, which are used to detect unreacted monomer, were used less routinely in 1982 when the first fractionation study of poly[11-(4'-cyanophenyl-4''-phenoxy)undecyl acrylate] was reported,³ the low-temperature tail in the DSC trace of their unfractionated polymer may be due to unreacted monomer. Figure 9 shows the effect of added monomer on the thermotropic behavior of linear polymer with high (DP_n = 70, pdi = 1.49) and low (DP_n = 10, pdi = 1.17) molecular weight. The low-molecular-weight polymer exhibits a single isotropization transition whose temperature (97 °C) and breadth (fwhm = 7.40 °C) appear to be unaffected, even when it is contaminated with up to 10% monomer. In this case, the isotropization temperatures of the monomer and polymer are similar. In contrast, the high-molecular-weight polymer (fwhm = 4.46 °C) contami-

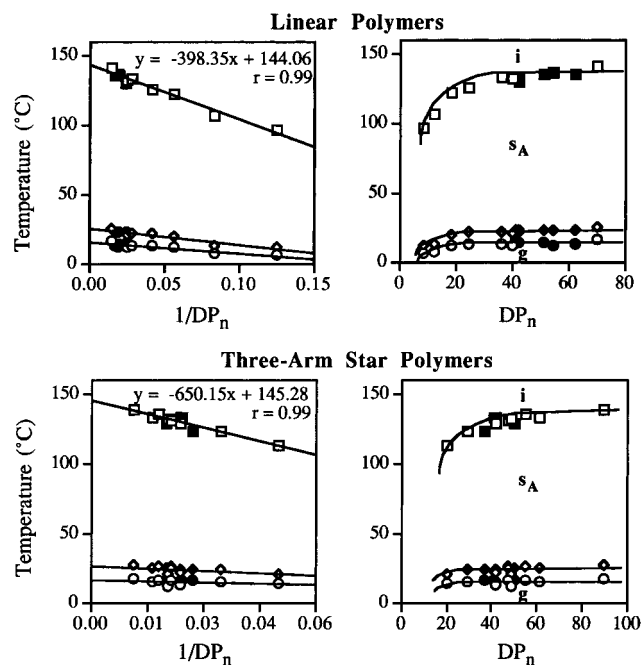


Figure 8. Dependence of the glass (○, ●), smectic C–smectic A (◇, ◆), and smectic A–isotropic (□, ■) phase transition temperatures of linear and 3-arm star poly[11-(4'-cyanophenyl-4''-phenoxy)undecyl acrylate]s prepared by ATRP (○, ◇, □) and their binary blends (●, ◆, ■) as a function of the number-average degree of polymerization and the inverse number-average degree of polymerization. Infinite molecular weight transitions: linear, *g* 16 *s_C* 26 *s_A* 144 *i*; 3-arm star, *g* 16 *s_C* 27 *s_A* 145 *i*.

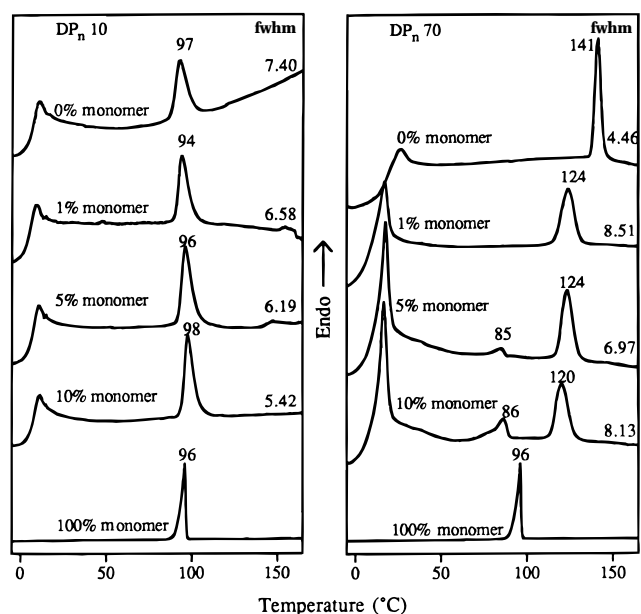


Figure 9. Normalized differential scanning calorimetry traces (10 °C/min) of poly[11-(4'-cyanophenyl-4''-phenoxy)undecyl acrylate] contaminated with varying amounts of 11-(4'-cyanophenyl-4''-phenoxy)undecyl acrylate; DP_n = 10 (pdi = 1.17) and DP_n = 70 (pdi = 1.49) prepared by ATRP; monomer scan is reduced relative to normalized polymer scans.

nated with only 1% monomer exhibits a broadened (fwhm = 8.52 °C) isotropization endotherm whose temperature is depressed by 17 °C relative to that of the pure polymer. If it is contaminated with 5–10% monomer, monomer partially phase separates from the polymer and exhibits a separate transition whose temperature is depressed by 10 °C relative to that of pure

monomer. The isotropization transition of the polymer is also broadened (fwhm = 6.97–8.13 °C) and depressed (17–21 °C) relative to that of the pure polymer. Therefore, residual monomer may be the cause of the low-temperature tailing in the isotropization transition of the unfractionated literature polymer.³

Binary Blends of Polymers Prepared by ATRP.

The polymer prepared by conventional radical polymerization has a broad monomodal, Gaussian-like molecular weight distribution and exhibits a very broad isotropization transition (fwhm = 16.5–17.0 °C). In contrast, both the highest molecular weight linear and 3-arm star polymers, which have monomodal most probable molecular weight distributions, exhibit extremely narrow isotropization transitions (fwhm = 4.46 °C). Therefore, a broad Gaussian-like distribution of chain lengths is not sufficient to broaden the breadth of the isotropization transition of poly[11-(4'-cyanophenyl-4''-phenoxy)undecyl acrylate]. Instead, the broad phase transition may be caused by an immiscible mixture of molecular architectures caused by chain branching at high monomer conversion in the conventional free-radical polymerization. That is, if the components of the polymer are immiscible in the mesophase, the transition should be either broadened or exhibit multiple maximums at the transition temperatures of the phase-segregated components, depending on their relative amounts and relative transition temperatures. If the components of the polymer are miscible, the polymer should exhibit a single, relatively narrow transition representing an average of the individual components.

This is demonstrated in Figures 10–12 by comparing the phase transitions of linear, linear/star, or 3-arm star binary blends to those of the corresponding unmixed samples. The two components of the unmixed samples were physically separated within the same DSC sample pan by a second sample pan,¹⁰ whereas the blends were created by co-dissolving the components in a minimum amount of THF and precipitating them in methanol at –78 °C. The exact compositions of the blends are listed in Table 5, along with their GPC-determined number-average degrees of polymerization and polydispersities. The average chain lengths of all of the blends are close to 50 repeat units (±13) and generally correspond to the expected values based on composition.

The binary blends of the linear polymers prepared by ATRP with DP_n = 40 (pdi = 1.30) and DP_n = 70 (pdi = 1.49) are monodisperse in molecular architecture but are the most polydisperse in molecular weight (pdi = 1.50–1.62) of the three types of blends. Figure 10 presents their DSC scans and those of the unmixed samples. The two linear polymers undergo isotropization at 133 °C and 141 °C. Figure 10 demonstrates that the phase-segregated, unmixed samples exhibit two isotropization maximums at 133 and 141 °C. Their relative areas correspond to the weight (or mole) ratio of the two components. In contrast, the corresponding binary blends of the two linear polymers exhibit a single *s_A*–*i* transition at an intermediate temperature. Although the isotropization temperatures of the three blends are essentially equal and therefore do not correspond exactly to their weight-averages (Table 5), they are within experimental error of the expected values. Therefore, the isotropization transitions, as well as the glass and *s_C*–*s_A* transitions of the blends, fit on the same molecular weight dependencies of the transition tem-

Table 5. Composition of Binary Blends of Poly[11-(4'-cyanophenyl-4''-phenoxy)undecyl acrylate]s Prepared by Atom Transfer Radical Polymerizations^a

architecture (DP _n /DP _n)	comp (%)		rec (%)	theor DP _n	GPC ^b		theor T _i ^c (°C)
	lower DP _n	higher DP _n			DP _n	pdi	
linear (40/70)	75	25	92	48	51	1.50	135
	50	50	88	55	54	1.62	137
	25	75	96	62	62	1.59	139
linear/star (36/42)	75	25	93	38	42	1.22	133
	50	50	92	39	41	1.21	132
	26	74	86	40	42	1.15	130
three-arm star (29/55)	75	25	98	36	37	1.31	126
	51	49	86	42	50	1.27	129
	23	77	99	49	47	1.31	132

^a Polymers were blended by dissolving in THF and precipitating with methanol. ^b Number-average degree of polymerization (DP_n) and polydispersity (pdi = M_w/M_n) determined by gel permeation chromatography (GPC) relative to polystyrene using a UV detector. ^c Weight-average T_i if miscible blend.

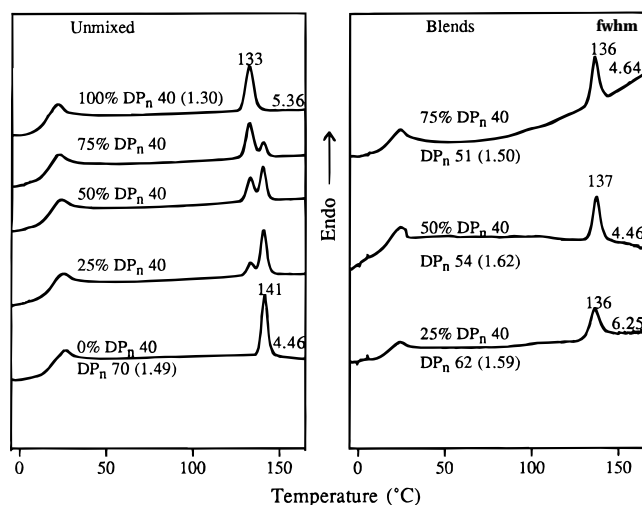


Figure 10. Normalized differential scanning calorimetry traces (10 °C/min) of binary unmixed (physically separated) composites and blends of linear poly[11-(4'-cyanophenyl-4''-phenoxy)undecyl acrylate]s (DP_n = 40, pdi = 1.30; DP_n = 70, pdi = 1.49) prepared ATRP.

temperatures in Figure 8 of the individual linear polymers. In addition, the breadth of the isotropization transitions of the blends is extremely narrow (fwhm = 4.46–6.25 °C) and does not cover the entire temperature range of isotropization of the two components. Therefore, the two linear components of these binary blends are miscible.

The binary blends of the linear (DP_n = 36, pdi = 1.34) and 3-arm star (DP_n = 42, pdi = 1.11) polymers prepared by ATRP are polydisperse in molecular architecture and monodisperse in molecular weight. However, the isotropization temperature of the 3-arm star polymer (129 °C) is lower than that of the linear polymer (134 °C). The DSC scans of the unmixed composites in Figure 11 clearly demonstrate that the lower temperature transition of a phase-segregated homopolymer may be due to a more branched polymer that is actually of higher molecular weight rather than to a lower molecular weight fraction. The relative areas of the two maximums at 129 and 134 °C correspond to the weight ratio of the two components. The corresponding binary blends exhibit a single, narrow (fwhm = 5.36–5.80 °C) isotropization transition at a temperature approximately equal to the weight-average temperature of the two components. Therefore, the linear and 3-arm star components of these binary blends are also miscible. This is consistent with recent calculations based on Flory–Huggins theory with entropic corrections that

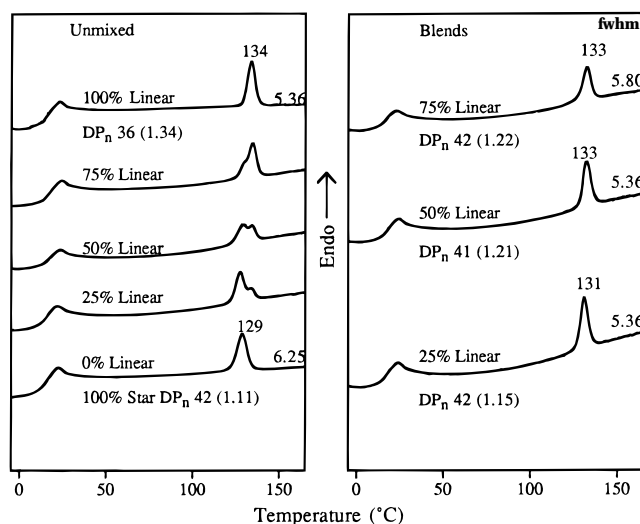


Figure 11. Normalized differential scanning calorimetry traces (10 °C/min) of binary unmixed (physically separated) composites and blends of linear (DP_n = 36, pdi = 1.34) and 3-arm star (DP_n = 42, pdi = 1.11) poly[11-(4'-cyanophenyl-4''-phenoxy)undecyl acrylate]s prepared ATRP.

predicts that 10–15 branch points are needed in a star polymer (DP_n = 100) to cause phase separation in a blend with linear polymer of DP_n = 100;⁴⁸ however, these calculations were not based on polymers that have a large side chain in each repeat unit. The theory also predicts that phase segregation in linear/branched polymer blends will be highest in mixtures of linear polymer with a low concentration of branched polymer.⁴⁸ This is consistent with the broader isotropization transition (fwhm = 5.80 °C) of the linear/star blend with only 25% star polymer compared to the other two blends (fwhm = 5.36 °C).

The binary blends of the 3-arm star polymers prepared by ATRP with DP_n = 29 (pdi = 1.24) and DP_n = 55 (pdi = 1.25) are monodisperse in molecular architecture and polydisperse in molecular weight. Figure 12 demonstrates that the phase-segregated, unmixed composites exhibit the two isotropization maximums (123 and 135 °C) of the two components in their relative weight ratios. The 3-arm star binary blends exhibit a single isotropization transition at approximately the weight-average temperature. All of their transition temperatures fit on the same molecular weight dependencies as those of the individual 3-arm star polymers (Figure 8). However, the isotropization transitions are significantly broader (fwhm = 8.93–15.2 °C) than those of either of the two components (fwhm = 5.36–7.14 °C).

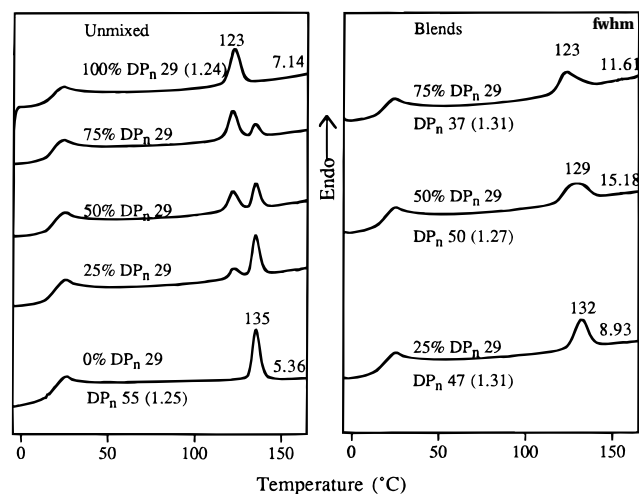


Figure 12. Normalized differential scanning calorimetry traces (10 °C/min) of binary unmixed (physically separated) composites and blends of 3-arm star poly[11-(4'-cyanophenyl-4''-phenoxy)undecyl acrylate]s ($DP_n = 29$, $pdi = 1.24$; $DP_n = 55$, $pdi = 1.25$) prepared ATRP.

That is, the breadth of the transition covers almost the entire temperature range of isotropization of the two components, which demonstrates that they do not mix well. Although both 3-arm star polymers have the same molecular architecture, they do not have the same branching density. The branching densities per 50 repeat units of the 3-arm star polymers are 1.7 branches when $DP_n = 29$, 1.2 branches when $DP_n = 42$, and 0.91 branch when $DP_n = 55$; the linear polymers have 0 branch/50 repeat units. Although the difference in branching density of the two components is slightly higher in the linear/star binary blends (1.2 branches/50 repeat units) than in the 3-arm star binary blends (0.79 branches/50 repeat units), this difference evidently becomes more significant as the overall branch content of the sample increases. This is consistent with the tendency of branched polyethylene blends to phase segregate.^{9,29,30} Therefore, branching is evidently the cause of the broad isotropization transitions of poly[11-(4'-cyanophenyl-4''-phenoxy)undecyl acrylate]s prepared by conventional radical polymerization. Similarly, the broad melting transition of LLDPE is due to its broad and multimodal distribution of short-chain branching density.¹¹

Isothermal Phase Segregation of Binary Blends of Polymers Prepared by ATRP. On the basis of the split isotropization transitions observed after isothermal annealing in the biphasic region followed by cooling to ambient temperature, previous researchers concluded that the biphasic region of MCLCPs¹⁷ and SCLCPs¹⁸ is due to selective partitioning of low- and high-molecular-weight fractions. Figure 13 demonstrates that the miscible 50/50 binary blend of linear poly[11-(4'-cyanophenyl-4''-phenoxy)undecyl acrylate]s prepared by ATRP can also be forced to phase segregate by annealing for as little as 1 h in the biphasic region at 134 °C. Isotropization is now split into the two maximums at 133 and 141 °C of the two linear components and covers their combined temperature range of isotropization. Phase segregation is essentially complete after 5–15 h.

The evolution of this phase segregation is shown by the polarized optical micrographs in Figure 14. Upon cooling from the isotropic melt to 134 °C, much of the material has organized into the S_A mesophase in the

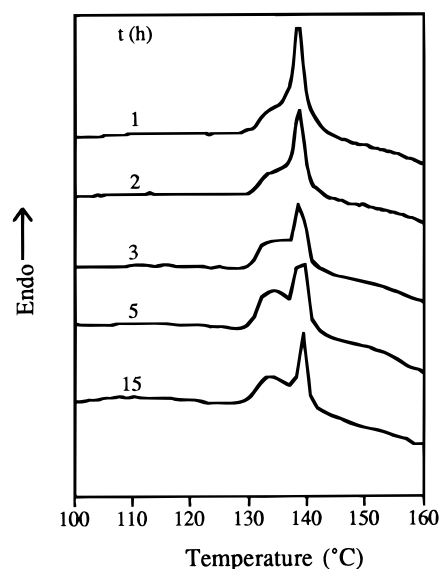


Figure 13. Normalized differential scanning calorimetry traces (10 °C/min) of the 50/50 binary blend of linear poly[11-(4'-cyanophenyl-4''-phenoxy)undecyl acrylate]s ($DP_n = 40$ and $DP_n = 70$) as a function of annealing time at 134 °C.

form of focal conic fans, although there are both large and small domains of the isotropic melt throughout the sample. After annealing for 15 min at 134 °C, the fan regions have grown and partially segregated from the isotropic domains, although the isotropic domains contain many anisotropic fans and bâtonnets. After annealing for 2 h at 134 °C, the fan regions have grown and segregated further from the isotropic domains, thereby decreasing the area occupied by the isotropic melt. Much of the anisotropic fans and bâtonnets within the isotropic domains have also coalesced and grown. After 6–15 h, the anisotropic fans are almost completely segregated into a continuous phase and the isotropic domains are smaller and almost free of bâtonnets.

As shown in Figure 15, the two components of all of the linear and linear/star binary blends can be forced to at least partially phase segregate by annealing in the biphasic region for 15 h. For example, the isotropization transitions of all of the linear binary blends are significantly broadened and split into two maximum, whereas only the linear/star blend with 25% star polymer exhibits two distinct maximums. Although the isotropization transitions of the 50/50 and 25/75 linear/star blends are not split into two clear maximum, the polarized optical micrograph in Figure 16 demonstrates that the 50/50 linear/star blend phase segregates in the same way as the 50/50 linear binary blend. However, comparison of the thermotropic behavior of the linear and linear/star binary blends to that of the corresponding unmixed composites in Figures 10 and 11 clearly demonstrates that the components of these blends are miscible and therefore exhibit a single, narrow isotropization transition under dynamic conditions.

In contrast, the 3-arm star binary blends, which exhibit broad isotropization transitions under dynamic conditions (Figure 12), do not readily phase segregate further. Only the isotropization transition of the 25/75 blend exhibits two distinct maximums after annealing at 130 °C in the biphasic region for 15 h. However, the isotropization transition of the 75/25 blend is depressed relative to the weight-average value, and the isotropization transition of the 50/50 blend is actually lower

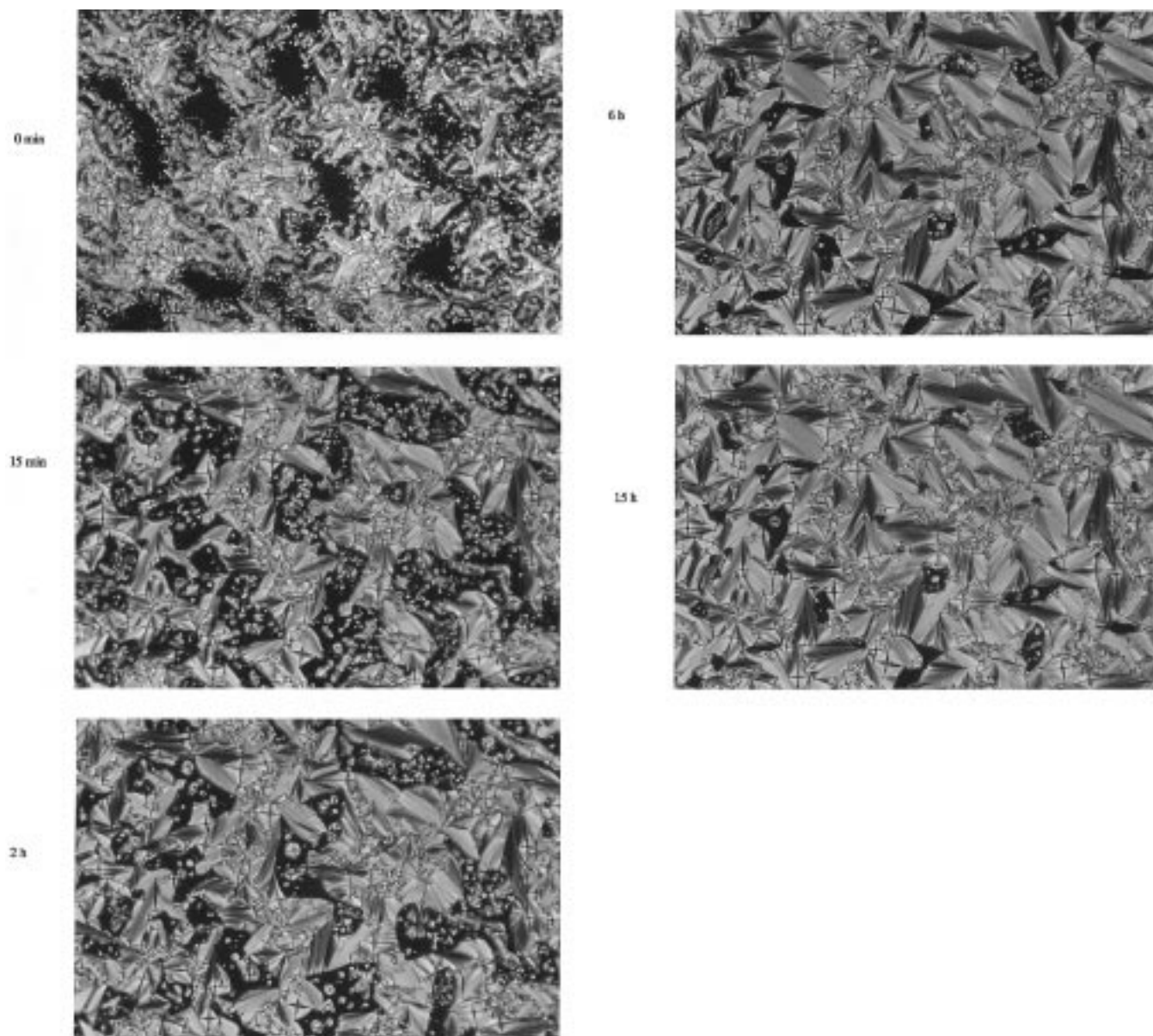


Figure 14. Polarized optical micrographs (200 \times) of the 50/50 binary blend of linear poly[11-(4'-cyanophenyl-4''-phenoxy)undecyl acrylate]s ($DP_n = 40$ and $DP_n = 70$) as a function of annealing time at 134 $^{\circ}\text{C}$ upon cooling from the isotropic melt.

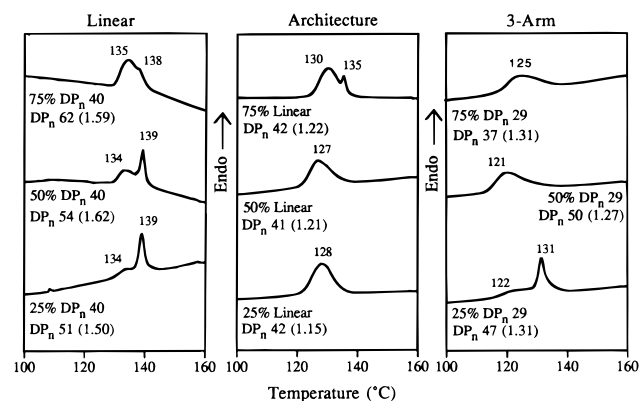


Figure 15. Normalized differential scanning calorimetry traces (10 $^{\circ}\text{C}/\text{min}$) of the linear ($DP_n = 40$ and $DP_n = 70$), linear ($DP_n = 36$)/3-arm star ($DP_n = 42$), and 3-arm star ($DP_n = 29$ and $DP_n = 55$) binary blends of poly[11-(4'-cyanophenyl-4''-phenoxy)undecyl acrylate]s after annealing for 15 h at 134, 130, and 130 $^{\circ}\text{C}$, respectively.

than those of either of the two components. Polarized optical microscopy confirms that the 50/50 3-arm star

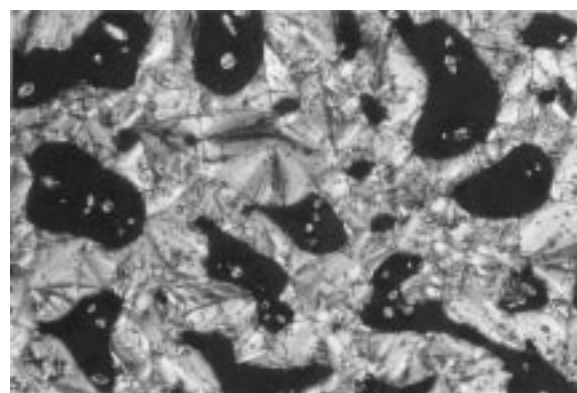


Figure 16. Polarized optical micrograph (200 \times) of the 50/50 binary blend of linear ($DP_n = 36$, $pdi = 1.34$) and 3-arm star ($DP_n = 42$, $pdi = 1.11$) poly[11-(4'-cyanophenyl-4''-phenoxy)undecyl acrylate]s prepared by ATRP after annealing at 130 $^{\circ}\text{C}$ for 15 h upon cooling from the isotropic melt.

binary blend is primarily isotropic after annealing at 130 $^{\circ}\text{C}$ for 15 h. As shown in Figure 17, anisotropic domains only persist after 15 h if the 50/50 blend is

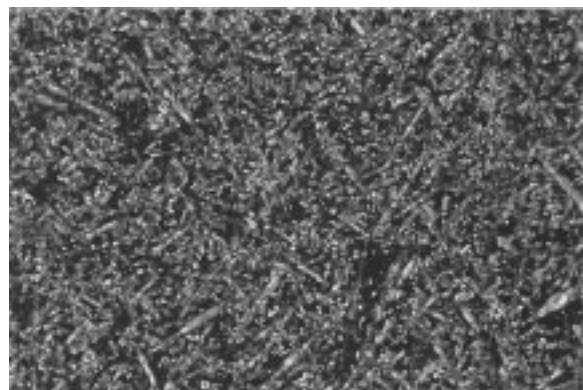
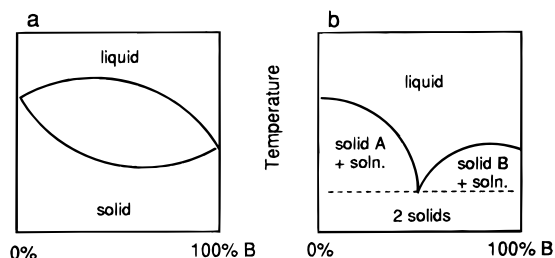


Figure 17. Polarized optical micrograph (200 \times) of the 51/49 binary blend of 3-arm star poly[11-(4'-cyanophenyl-4''-phenoxy)undecyl acrylate]s ($DP_n = 29$, $pdi = 1.24$; $DP_n = 55$, $pdi = 1.25$) prepared ATRP after annealing at 126 $^{\circ}\text{C}$ for 15 h upon cooling from the isotropic melt.

Chart 2. (a) Phase diagrams of a Mixture with Complete Miscibility in Both Liquid and Solid Phases; (b) a Mixture with Complete Miscibility in the Liquid Phase and Complete Immiscibility in the Solid Phase.⁴⁹



annealed at 126 $^{\circ}\text{C}$ or less, although the isotropic domains are very small due to the large number of defects. This indicates that the polymer chains do not readily diffuse through the more immiscible systems.

The lower isotropization temperature of the 50/50 blend provides further evidence that the components of the 3-arm star binary blends do not mix well in the s_A mesophase. As shown in Chart 2a by the phase diagram of a mixture that is completely miscible in both the liquid and solid states, the transition temperature is intermediate between those of the two components.⁴⁹ In contrast, the transition temperatures of a mixture that is completely miscible in the liquid phase but completely immiscible in the solid state (Chart 2b), are depressed relative to that of at least one of the two components, with the lowest transition temperature at the eutectic composition.⁴⁹ The other compositions have large melt/biphasic regions. Therefore, both the isothermal annealing and dynamic studies of the binary blends indicate that the 3-arm star polymers tend to be miscible in the isotropic melt but immiscible in the s_A mesophase; the linear binary blends are apparently miscible in both the isotropic melt and s_A mesophase. That is, if the polymer chains are homogeneous in both the isotropic melt and the mesophase, rapid cooling favors comixing in the mesophase, whereas slow cooling through the biphasic region favors diffusion and segregation of two fractions with significantly different molecular weights and/or branching densities. However, if the two components have limited miscibility in the mesophase, they form a much greater number of defects (domain boundaries) within the biphasic region, thereby hindering macroscopic segregation. Therefore, the ability to fractionate SCLCPs in the biphasic region

indicates that all of the components are miscible and therefore diffusive in both the isotropic melt and the mesophase.

Conclusions

Atom transfer radical polymerization can be used to study structure/property relationships of poly[11-(4'-cyanophenyl-4''-phenoxy)undecyl acrylate] and other SCLCPs. However, it is difficult to attain complete conversion of either the linear or 3-arm star poly[11-(4'-cyanophenyl-4''-phenoxy)undecyl acrylate]s when the attempted degrees of polymerization are greater than 60 ($[M]_0/[I]_0 > 60$). Residual copper must be stringently removed to prevent decomposition of the chain ends and sometimes broadening of their phase transitions. Even in the absence of copper, the alkyl bromide chain ends are less stable than those synthesized by conventional free-radical polymerizations using AIBN as the initiator. Therefore, ATRP is most useful for synthesizing SCLCPs with lower transition temperatures.

In contrast to lattice theory of rodlike molecules with a mixture of axial ratios,²³ the biphasic regions of the binary blends of linear poly[11-(4'-cyanophenyl-4''-phenoxy)undecyl acrylate] are not broader than those of either of the two components. Similarly, the biphasic regions of the linear and 3-arm star polymers with most probable distributions of chain lengths are not broader than those of the corresponding polymers with Poisson distributions. Therefore, poly[11-(4'-cyanophenyl-4''-phenoxy)undecyl acrylate] behaves as a system that is monodisperse in rod length. This indicates that SCLCPs can be considered as a mixture of monodisperse rods (mesogenic side chains) and random coils (distorted⁵⁰ polymer backbone).²⁴ In this case, lattice theory predicts that the addition of the random coil broadens the biphasic region of the monodisperse rod,⁵¹ which accounts for the slightly broader phase transitions of well-defined SCLCPs compared to those of low-molar-mass liquid crystals. Therefore, the extremely broad isotropization transitions of many SCLCPs prepared by standard radical polymerizations cannot be accounted for simply by a broad polydispersity in molecular weight. The limited miscibility and broad isotropization transitions of the binary mixtures of the 3-arm star polymers indicate that the broad isotropization transitions of SCLCPs prepared by standard radical polymerizations are due to a mixture of branched structures which result from chain transfer to polymer at high monomer conversion.

Experimental Section

Materials. Acryloyl chloride (96%), 1-bromohexane (98%), 11-bromo-1-undecanol (98%), 1-decanethiol (96%), 4'-hydroxy-4-biphenylcarbonitrile (97%), methyl 2-bromopropionate (97%), and 2,4,6-tris(bromomethyl)mesitylene (98%) were used as received from Aldrich. Azobisisobutyronitrile (AIBN, Johnson Mathey, 99%) was recrystallized from methanol below 40 $^{\circ}\text{C}$. Cuprous bromide (Alfa, 98%) and 4,4'-dimethyl-2,2'-dipyridyl (Fluka, 99%) were used as received. Triethylamine (Baker) was stirred over KOH and distilled under N_2 . Benzene was washed sequentially with concentrated H_2SO_4 and water, stored over $CaCl_2$, and distilled from CaH_2 under N_2 . Reagent-grade tetrahydrofuran (THF) was dried by distillation from purple sodium benzophenone ketyl under N_2 . Stock solutions of methanolic ammonium chloride containing 45 mL of methanol and 15 mL saturated NH_4Cl were prepared to removed copper salts from ATRP polymers by precipitations at -78°C ; water was necessary to keep NH_4Cl in solution at low

temperature. All other reagents and solvents were commercially available and used as received.

Techniques. All reactions were performed under a N₂ atmosphere using a Schlenk line unless noted otherwise. ¹H NMR spectra (δ, ppm) were recorded on either a Bruker AC-200 (200 MHz) or a Bruker AM-300 (300 MHz) spectrometer. Unless noted otherwise, all spectra were recorded in CDCl₃ with TMS as an internal standard. Relative molecular weights were determined by gel permeation chromatography (GPC) at 35 °C using THF as solvent (1.0 mL/min), a set of 50, 100, 500, and 10⁴ Å and linear (50–10⁴ Å) Styragel 5-μm columns, a Waters 486 tunable UV/visible detector set at 300 nm, and a Waters 410 differential refractometer.

All polymers and their blends were dried overnight in vacuo at room temperature and then at 60 °C for 2 h before their thermotropic behavior was analyzed. A Perkin-Elmer DSC-7 differential scanning calorimeter was used to determine the thermal transitions that were read as the maximum or minimum of the endothermic or exothermic peaks, respectively. Glass transition temperatures (*T*_g's) were read as the middle of the change in heat capacity. All heating and cooling rates were 10 °C/min. Both enthalpy changes and transition temperatures were calibrated using indium and zinc standards. TGA were conducted with a Perkin-Elmer TGA-7 at a heating rate of 10 °C/min under air. The onset of the decomposition temperature was calculated by extrapolation of the constant-weight region to the tangent of the weight loss. A Leitz Laborlux 12 Pol S polarized optical microscope (magnification 200×) equipped with a Mettler FP82 hot stage and a Mettler FP90 central processor was used to analyze the thermal transitions and anisotropic textures. Thin samples were prepared by melting a minimum amount of compound between a clean glass slide and a cover slip and rubbing the cover slip with a spatula. The breadth of the isotropization transitions was measured by cooling from the isotropic melt at 10 °C/min and recording the temperature at the first appearance of brightness and at the last detection of motion; each value is the mean of three measurements.

Synthesis of Monomer and Precursors. 11-(4'-Cyanophenyl-4''-phenoxy)undecanol. 11-(4'-Cyanophenyl-4''-phenoxy)undecanol was prepared in 61–86% yield as in the following example. A solution of 11-bromo-1-undecanol (8.1 g, 32 mmol) in ethanol (40 mL) was added dropwise over 1.5 h to a refluxing solution of 4'-hydroxy-4-biphenylcarbonitrile (6.0 g, 31 mmol) and K₂CO₃ (4.7 g, 34 mmol) in ethanol (40 mL) and water (10 mL). After refluxing for 25 h, the reaction was poured into water. The precipitate was collected and recrystallized from ethanol to yield 9.7 g (86%) of 11-(4'-cyanophenyl-4''-phenoxy)undecanol as white crystals. ¹H NMR: δ 1.31 (m, [CH₂]₆), 1.49 (m, CH₂CH₂CH₂OAr), 1.59 (m, CH₂CH₂OH), 1.83 (m, CH₂CH₂OAr), 3.64 (t, CH₂OH), 4.00 (t, OCH₂), 6.99 (d, 2 aromatic H *ortho* to OCH₂), 7.52 (d, 2 aromatic H *meta* to OCH₂), 7.66 (m, 4 aromatic H *ortho* and *meta* to CN).

11-(4'-Cyanophenyl-4''-phenoxy)undecyl acrylate. 11-[(4'-Cyanophenyl-4''-phenoxy)undecyl] acrylate was prepared in 56–97% yield as in the following example. A solution of acryloyl chloride (2.6 g, 39 mmol) in dry THF (30 mL) was added dropwise over 30 min to an ice-cooled solution of 4-[(hydroxyundecyl)oxy]-4'-cyanobiphenyl (9.6 g, 26 mmol) and dry NEt₃ (4.5 g, 45 mmol) in dry THF (500 mL). The reaction was warmed to room temperature, stirred for 16 h, and then poured into water (500 mL). The resulting precipitate was filtered and recrystallized from a mixture of ethanol (100 mL) and toluene (5 mL) to yield 6.1 g (56%) of 11-(4'-cyanophenyl-4''-phenoxy)undecyl acrylate as white crystals. ¹H NMR: δ 1.31 (m, [CH₂]₇), 1.67 (m, CH₂CH₂OAr), 1.81 (m, CH₂CH₂O₂C), 4.00 (t, CH₂OAr), 4.15 (t, CH₂O₂C), 5.81 (dd, 1 olefinic H *trans* to CO₂), 6.10 (dd, 1 olefinic H *gem* to CO₂), 6.40 (dd, 1 olefinic H *cis* to CO₂), 6.99 (d, 2 aromatic H *ortho* to OCH₂), 7.53 (d, 2 aromatic H *meta* to OCH₂), 7.68 (m, 4 aromatic H *ortho* and *meta* to CN).

Synthesis of Ligand. 4,4'-Diheptyl-2,2'-dipyridyl. 4,4'-Diheptyl-2,2'-dipyridyl was prepared in 16–56% yield as in the following example. A solution of lithium diisopropylamide

(7.1 g, 66 mmol) in dry THF (20 mL) was prepared under a N₂ atmosphere in a Vacuum Atmospheres drybox. The closed reaction flask was removed from the drybox, attached to a Schlenk line under N₂, and cooled to –78 °C in an acetone/CO₂ bath. A solution of 4,4'-dimethyl-2,2'-dipyridyl (4.8 g, 26 mmol) in dry THF (110 mL) was added dropwise over 10 min to the reaction mixture, and then 1-bromohexane (8.6 mL, 61 mmol) was added via a syringe. The reaction was allowed to warm to room temperature and was stirred for 20 h. The reaction was quenched with water (100 mL), the organic layer was separated, and the solvent was removed by rotary evaporation. The resulting solid was passed through a column of neutral alumina, using Et₂O/hexanes (12:1) as the eluant, and recrystallized from acetonitrile (80 mL) to yield 5.2 g (56%) of 4,4'-diheptyl-2,2'-dipyridyl as white needles. ¹H NMR: δ 0.86 (t, CH₃, 6 H), 1.28 (m, [CH₂]₄, 16 H), 1.69 (m, CH₂CH₂Ar, 4 H), 2.7 (t, CH₂Ar, 4 H), 7.18 (d, 2 aromatic H *para* to Ar), 8.29 (s, 2 aromatic H *ortho* to Ar), 8.58 (d, 2 aromatic H *meta* to Ar).

Synthesis of Polymer by Conventional Free-Radical Polymerization. A mixture of 11-(4'-cyanophenyl-4''-phenoxy)undecyl acrylate (1.1 g, 2.5 mmol) and AIBN (8.0 mg, 49 μmol) in dry benzene (11 mL) was degassed in a sealable tube. The tube was then sealed under vacuum and stirred at 60 °C for 29 h. The polymer was diluted with THF (3 mL), precipitated into cold (–78 °C) methanol (75 mL), and collected. According to GPC, the crude product contained 83% polymer and 17% unreacted monomer. In order to remove monomer, the polymer was reprecipitated three times from THF (4–10 mL) into a warm (50 °C) solution of ethanol (60–80 mL) and toluene (0–15 mL), which was cooled first to room temperature and then to –78 °C prior to collecting the precipitate. The combined filtrate from these precipitations was concentrated to recover additional precipitate of oligomeric material, which was added to the polymer sample to yield 0.77 g (72%) of poly-[11-(4'-cyanophenyl-4''-phenoxy)undecyl acrylate] as a hard solid; *M*_n = 2.52 × 10⁴, *pdi* = 3.43.

Fractionation of Polymer by Conventional Free-Radical Polymerization. Methanol was added dropwise to a dilute solution of poly[11-(4'-cyanophenyl-4''-phenoxy)undecyl acrylate] (0.4889 g, *M*_n = 2.52 × 10⁴, *pdi* = 3.43) in THF (100 mL) until the solution became cloudy (150 mL of methanol). The solution was allowed to settle overnight, and the precipitate was collected. This large fraction (>0.1 g) was redissolved in THF (50 mL), and methanol was added dropwise until the solution became cloudy (75 mL). The precipitate was collected to yield 250 mg (5%) of fraction 1 (Table 1); *M*_n = 4.31 × 10⁴, *pdi* = 1.57. The solvent from this filtrate was removed by rotary evaporation to yield 0.1074 g (22%) of fraction 2; *M*_n = 2.95 × 10⁴, *pdi* = 1.75. The next four fractions were obtained by adding methanol dropwise to the filtrate from the first precipitate that contained fractions 1 and 2 until it became cloudy: 710 mg (14%) of fraction 3 after 100 mL of methanol was added, *M*_n = 2.40 × 10⁴, *pdi* = 1.96; 0.1083 g (22%) of fraction 4 after another 125 mL of methanol was added, *M*_n = 2.09 × 10⁴, *pdi* = 1.74; 209 mg (4%) of fraction 5 after another 50 mL of methanol was added, *M*_n = 1.20 × 10⁴, *pdi* = 2.04; 477 mg (10%) of fraction 6 after another 75 mL of methanol was added, *M*_n = 8.63 × 10³, *pdi* = 1.78. The solvent from the filtrate of fraction 6 was removed by rotary evaporation, and the resulting viscous yellow oil was reprecipitated from THF (2 mL) into methanol (40 mL) to yield 268 mg (7%) of fraction 7 as a sticky solid; *M*_n = 5.79 × 10³, *pdi* = 1.92; ¹H NMR confirmed that fraction 7 contained only poly[11-(4'-cyanophenyl-4''-phenoxy)undecyl acrylate].

Synthesis of Low-Molecular-Weight Polymer by Conventional Free-Radical Polymerization Using a Chain-Transfer Agent. A mixture of 11-(4'-cyanophenyl-4''-phenoxy)undecyl acrylate (1.0 g, 2.5 mmol), 1-decanethiol (19 mg, 0.11 mmol), and AIBN (20 mg, 0.12 mmol) in dry benzene (2.5 mL) was degassed in a sealable tube. The tube was then sealed under vacuum and stirred at 60 °C for 28 h. The polymer was precipitated from THF (2 mL) into cold (–78 °C) methanol (50 mL) to yield 0.94 g (90%) of poly[11-(4'-cyanophenyl-4''-phenoxy)undecyl acrylate] as a sticky solid; *M*_n = 9.8 × 10³,

$DP_n = 23$, $pdi = 1.53$. Methanol was added dropwise to a dilute solution of this polymer in THF (150 mL) until the solution became cloudy (275 mL). After settling, the precipitate was collected. The solvent from this filtrate was removed by rotary evaporation to yield a sticky yellow solid. This solid was dissolved in THF (3 mL) and precipitated into cold (-78°C) methanol (50 mL) to yield 0.22 g (21%) of poly[11-(4'-cyanophenyl-4''-phenoxy)undecyl acrylate] as a sticky solid; $M_n = 4.89 \times 10^3$, $DP_n = 11$, $pdi = 1.20$.

Synthesis of the Linear Polymer Used To Study the Effect of Residual Copper from ATRP. A mixture of 11-(4'-cyanophenyl-4''-phenoxy)undecyl acrylate (1.0 g, 2.4 mmol), methyl 2-bromopropionate (81 mg, 0.49 mol), CuBr (70 mg, 0.49 mmol), and 4,4'-diheptyl-2,2'-dipyridyl (0.51 g, 1.4 mmol) was degassed in a sealable tube. The tube was then sealed under vacuum and stirred at 100°C for 1.2 h. The polymer was precipitated in cold (-78°C) methanol (75 mL) and collected, and a small amount was reserved for analysis. The remaining polymer was reprecipitated four times from THF (4 mL) into cold (-78°C) 3:9 saturated aqueous NH_4Cl /methanol (60–75 mL), each time reserving a small amount of the precipitate for analysis. One additional precipitation from THF (3 mL) into cold (-78°C) methanol (60 mL) yielded 0.66 g (66%) of poly[11-(4'-cyanophenyl-4''-phenoxy)undecyl acrylate] as a sticky white solid; $M_n = 4.57 \times 10^3$, $pdi = 1.17$.

Synthesis of Linear Polymers by ATRP. Linear polymers were prepared by ATRP in 45–84% yield as in the following example. A mixture of 11-(4'-cyanophenyl-4''-phenoxy)undecyl acrylate (0.54 g, 1.3 mmol), methyl 2-bromopropionate (21 mg, 0.13 mmol), CuBr (18 mg, 0.13 mmol) and 4,4'-diheptyl-2,2'-dipyridyl (0.14 g, 0.39 mmol) was degassed in a sealable tube. The tube was then sealed under vacuum and stirred at 100°C for 1.2 h. The polymer was precipitated in cold (-78°C) methanol (50 mL), collected, and purified by reprecipitating once from THF (4 mL) into cold (-78°C) methanol (50 mL), twice from THF (4 mL) into cold (-78°C) 3:9 saturated aqueous NH_4Cl /methanol (15 mL), and then one additional precipitation from THF (4 mL) into cold (-78°C) methanol (50 mL) to yield 0.39 g (70%) of poly[11-(4'-cyanophenyl-4''-phenoxy)undecyl acrylate] as a sticky solid; $M_n = 5.05 \times 10^3$, $pdi = 1.16$.

Synthesis of Three-Arm Star Polymers by ATRP. Three-arm star polymers were prepared by ATRP in 22–85% yield as in the following example. A mixture of 11-(4'-cyanophenyl-4''-phenoxy)undecyl acrylate (0.50 g, 1.2 mmol), 2,4,6-tris(bromomethyl)mesitylene (32 mg, 80 μmol), CuBr (34 mg, 0.23 mmol), and 4,4'-diheptyl-2,2'-dipyridyl (0.26 g, 0.72 mmol) in dry benzene (0.5 mL) was degassed in a sealable tube. The tube was then sealed under vacuum and stirred at 100°C for 3 h. The polymer was precipitated into cold (-78°C) methanol (50 mL), collected, and purified by sequentially reprecipitating from THF (4 mL) into cold (-78°C) methanol (50 mL), twice from THF (4 mL) into cold (-78°C) 3:9 saturated aqueous NH_4Cl /methanol (15 mL), and then one additional precipitation from THF (4 mL) into cold (-78°C) methanol (50 mL) to yield 0.34 g (67%) of poly[11-(4'-cyanophenyl-4''-phenoxy)undecyl acrylate] as a sticky solid; $M_n = 8.68 \times 10^3$, $pdi = 1.15$.

Preparation of Binary Polymer Blends. Binary polymer blends were prepared in 86–99% yield. In a typical procedure, a cold (-78°C) solution of concd HCl (2 drops) in methanol (50 mL) was added dropwise to a solution of $DP_n = 39$ linear polymer (9.9 mg) and $DP_n = 70$ linear polymer (10 mg) in a minimum amount of THF (<0.5 mL) until a white precipitate formed (~ 2 mL). The precipitate was collected to yield 18 mg (88%) of the 50/50 linear binary blend as a sticky white solid; $M_n = 2.27 \times 10^4$, $pdi = 1.62$.

Acknowledgment is made to the University of Michigan for a Rackham Faculty Grant for providing seed money for this research. C.P. also acknowledges the National Science Foundation for an NSF Young Investigator Award (1994–1999) and matching funds from Bayer, Dow Chemical, DuPont (DuPont Young

Professor Grant), GE Foundation (GE Junior Faculty Fellowship), Pharmacia Biotech, and Waters Corp. A.M.H. acknowledges the University of Michigan for a Smeaton Fellowship for undergraduate research. A.M.K. acknowledges the University of Michigan for a Crutcheon Research Grant and an Otto Graf Research Award for undergraduates, and the National Science Foundation for an REU (Research Experience for Undergraduates). Preliminary results from this paper were presented by A.M.K. at the 1997 Waldo Semon Undergraduate Research Award Symposium at the University of Akron.

References and Notes

- (1) (a) Sagane, T.; Lenz, R. W. *Polym. J.* **1988**, *20*, 923. (b) Sagane, T.; Lenz, R. W. *Polymer* **1989**, *30*, 2269. (c) Sagane, T.; Lenz, R. W. *Macromolecules* **1989**, *22*, 3763.
- (2) Héroguez, V.; Schappacher, M.; Papon, E.; Deffieux, A. *Polym. Bull.* **1991**, *25*, 307; $pdi = 1.9$, prepared directly by cationic polymerization of the mesogenic vinyl ether; $pdi = 1.2$, prepared by quantitative etherification of poly[*n*-(chloroalkyl)-vinyl ether] precursor polymers.
- (3) Kostromin, S. G.; Talroze, R. V.; Shibaev, V. P.; Platé, N. A. *Makromol. Chem., Rapid Commun.* **1982**, *3*, 803.
- (4) Pugh, C.; Kiste, A. L. *Prog. Polym. Sci.* **1997**, *22*, 601.
- (5) Komiya, Z.; Pugh, C.; Schrock, R. R. *Macromolecules* **1992**, *25*, 3609.
- (6) We are using the number of branches per 50 repeat units in order to compare directly to SCLCPs, which are typically synthesized with ~ 50 repeat units.
- (7) See, for example: Odian, G. *Principles of Polymerization*, 3rd ed.; Wiley-Interscience: New York, 1991.
- (8) Alamo, R. G.; Viers, B. D.; Mandelkern, L. *Macromolecules* **1995**, *28*, 3205.
- (9) Wignall, G. D.; Londono, J. D.; Lin, J. S.; Alamo, R. G.; Galante, M. J.; Mandelkern, L. *Macromolecules* **1995**, *28*, 3156.
- (10) Joskowicz, P. L.; Muñoz, A.; Barrera, J.; Müller, A. J. *Macromol. Chem. Phys.* **1995**, *196*, 385.
- (11) Liu, T. M.; Harrison, I. R. *Thermochim. Acta* **1994**, *233*, 167.
- (12) Gerum, W.; Höhne, G. W. H.; Wilke, W.; Arnold, M.; Wegner, T. *Macromol. Chem. Phys.* **1996**, *197*, 1691.
- (13) Alamo, R. G.; Chan, E. K. M.; Mandelkern, L.; Voigt-Martin, I. G. *Macromolecules* **1992**, *25*, 6381.
- (14) Alamo, R. G.; Mandelkern, L. *Macromolecules* **1991**, *24*, 6480.
- (15) Tashiro, K.; Stein, R. S.; Hsu, S. L. *Macromolecules* **1992**, *25*, 1801.
- (16) (a) Tashiro, K.; Izuchi, M.; Kaneuchi, F.; Jin, C.; Kobayashi, M.; Stein, R. S. *Macromolecules* **1994**, *27*, 1240. (b) Tashiro, K.; Imanishi, K.; Izumi, Y.; Kobayashi, M.; Kobayashi, K.; Satoh, M.; Stein, R. S. *Macromolecules* **1995**, *28*, 8477.
- (17) (a) d'Allest, J. F.; Wu, P. P.; Blumstein, A.; Blumstein, R. B. *Mol. Cryst. Liq. Cryst. Lett.* **1986**, *3*, 103. (b) d'Allest, J. F.; Sixou, P.; Blumstein, A.; Blumstein, R. B. *Mol. Cryst. Liq. Cryst.* **1988**, *157*, 229. (c) Kim, D. Y.; d'Allest, J. F.; Blumstein, A.; Blumstein, R. B. *Mol. Cryst. Liq. Cryst.* **1988**, *157*, 253. (d) Esnault, P.; Gauthier, M. M.; Volino, F.; d'Allest, J. F.; Blumstein, R. B. *Mol. Cryst. Liq. Cryst.* **1988**, *157*, 273. (e) Laus, M.; Angeloni, A. S.; Galli, G.; Chiellini, E. *Macromolecules* **1992**, *25*, 5901. (f) Nakai, A.; Wang, W.; Hashimoto, T.; Blumstein, A.; Maeda, Y. *Macromolecules* **1994**, *27*, 6964. (g) Nakai, A.; Wang, W.; Hashimoto, T.; Blumstein, A. *Macromolecules* **1996**, *29*, 5288.
- (18) (a) Galli, G.; Chiellini, E.; Laus, M.; Caretti, D.; Angeloni, A. S. *Makromol. Chem., Rapid Commun.* **1991**, *12*, 43. (b) Laus, M.; Angeloni, A. S.; Galli, G.; Chiellini, E. *Thermochim. Acta* **1993**, *227*, 49. (c) Sarna, R. J.; Simon, G. P.; Day, G.; Kim, H.-J.; Jackson, W. R. *Macromolecules* **1994**, *27*, 1603.
- (19) Galli, G.; Chiellini, E.; Laus, M.; Angeloni, A. S.; Francescangeli, O.; Yang, B. *Macromolecules* **1994**, *27*, 303.
- (20) Flory, P. J. *Adv. Polym. Sci.* **1984**, *59*, 1.
- (21) Discussions from: *Faraday Discuss. Chem. Soc.* **1985**, 85–100.
- (22) (a) Flory, P. J. *Macromolecules* **1978**, *11*, 1141. (b) Khokhlov, A. R.; Semenov, A. N. *Macromolecules* **1986**, *19*, 373.

- (23) (a) Flory, P. J.; Abe, A. *Macromolecules* **1978**, *11*, 1119. (b) Abe, A.; Flory, P. J. *Macromolecules* **1978**, *11*, 1122. (c) Flory, P. J.; Frost, R. S. *Macromolecules* **1978**, *11*, 1126. (d) Frost, R. S.; Flory, P. J. *Macromolecules* **1978**, *11*, 1134. (e) Moscicki, J. K.; Williams, G. *Polymer* **1982**, *23*, 558.
- (24) According to Flory,²⁰ "A special class of polymeric liquid crystals is obtained by attaching rigid side chains to a flexible backbone. Inasmuch as it is the side chains that engage in formation of the liquid crystalline domains, these systems are more closely akin to low molecular weight liquid crystals."
- (25) If chain transfer occurs at either a lateral site on the mesogen or within the mesogen (e.g., azobenzene-, stilbene-, and benzylidene aniline-based mesogens), a theory that considers imperfections in the rigid rod may apply and should be considered simultaneously with the problems of limited miscibility of branched structures. If a system has only imperfectly rigid rods with a blocklike rigidity, a nematic-isotropic biphasic region should not broaden.²⁶
- (26) Matheson, R. R., Jr.; Flory, P. J. *Macromolecules* **1981**, *14*, 954.
- (27) Lu, L.; Alamo, R. G.; Mandelkern, L. *Macromolecules* **1994**, *27*, 6571.
- (28) Hill, M. J.; Barham, P. J. *Polymer* **1995**, *36*, 1523.
- (29) Minick, J.; Moet, A.; Baer, E. *Polymer* **1995**, *36*, 1923.
- (30) Alamo, R. G.; Londono, J. D.; Mandelkern, L.; Stehling, F. C.; Wignall, G. D. *Macromolecules* **1994**, *27*, 411.
- (31) (a) Freed, K. F.; Dudowicz, J. *Macromolecules* **1996**, *29*, 625. (b) Graessley, W. W.; Krishnamoorti, R.; Balsara, N. P.; Butera, R. J.; Fetters, L. J.; Lohse, D. J.; Schulz, D. N.; Sissano, J. A. *Macromolecules* **1994**, *27*, 3896.
- (32) Alamo, R. G.; Graessley, W. W.; Krishnamoorti, R.; Lohse, D. J.; Londono, J. D.; Mandelkern, L.; Stehling, F. C.; Wignall, G. D. *Macromolecules* **1997**, *30*, 561.
- (33) (a) Tashiro, K.; Satkowski, M. M.; Stein, R. S.; Li, Y.; Chu, B.; Hsu, S. L. *Macromolecules* **1992**, *25*, 1809. (b) Tashiro, K.; Izuchi, M.; Kobayashi, M.; Stein, R. S. *Macromolecules* **1994**, *27*, 1221. (c) Tashiro, K.; Izuchi, M.; Kobayashi, M.; Stein, R. S. *Macromolecules* **1994**, *27*, 1228. (d) Tashiro, K.; Izuchi, M.; Kobayashi, M.; Stein, R. S. *Macromolecules* **1994**, *27*, 1234. (e) Tashiro, K.; Imanishi, K.; Izuchi, M.; Kobayashi, M.; Ito, Y.; Imai, M.; Yamaguchi, Y.; Ohashi, M.; Stein, R. S. *Macromolecules* **1995**, *28*, 8484.
- (34) Londono, J. D.; Narten, A. H.; Wignall, G. D.; Honnell, K. G.; Hsieh, E. T.; Johnson, T. W.; Bates, F. S. *Macromolecules* **1994**, *27*, 2864.
- (35) (a) Nesarikar, A.; Crist, B.; Davidovich, A. *J. Polym. Sci., Polym. Phys. Ed.* **1994**, *32*, 641. (b) Wignall, G. D.; Alamo, R. G.; Londono, J. D.; Mandelkern, L.; Stehling, F. C. *Macromolecules* **1996**, *29*, 5332.
- (36) (a) Veregin, R. P. N.; Odell, P. G.; Michalak, L. M.; Georges, M. K. *Macromolecules* **1996**, *29*, 2746 and references therein. (b) Hawker, C. J.; Barclay, C. G.; Dao, J. *J. Am. Chem. Soc.* **1996**, *118*, 11467 and references therein. (c) Fukuda, T.; Terauchi, T.; Goto, A.; Ohno, K.; Tsujii, Y.; Miyamoto, T.; Kobatake, S.; Yamada, B. *Macromolecules* **1996**, *29*, 6393. (d) Greszta, D.; Matyjaszewski, K. *Macromolecules* **1996**, *29*, 7661.
- (37) (a) Percec, V.; Barboiu, B. *Macromolecules* **1995**, *28*, 7970. (b) Percec, V.; Barboiu, B.; Neumann, A.; Ronda, J. C.; Zhao, M. *Macromolecules* **1996**, *29*, 3665.
- (38) (a) Wang, J. S.; Matyjaszewski, K. *J. Am. Chem. Soc.* **1995**, *117*, 5614. (b) Matyjaszewski, K.; Patten, T. E.; Xia, J. *J. Am. Chem. Soc.* **1997**, *119*, 674.
- (39) Wang, J.-S.; Matyjaszewski, K. *Macromolecules* **1995**, *28*, 7572.
- (40) (a) Wang, J.-S.; Matyjaszewski, K. *Macromolecules* **1995**, *28*, 7901. (b) Patten, T. E.; Xia, J.; Abernathy, T.; Matyjaszewski, K. *Science* **1996**, *272*, 866.
- (41) (a) Kato, M.; Kamigaito, M.; Sawamoto, M.; Higashimura, T. *Macromolecules* **1995**, *28*, 1721. (b) Ando, T.; Kato, M.; Kamigaito, M.; Sawamoto, M. *Macromolecules* **1996**, *29*, 1070. (c) Matsuyama, M.; Kamaigaito, M.; Sawamoto, M. *J. Polym. Sci., Polym. Chem. Ed.* **1996**, *34*, 3585. (d) Kotani, Y.; Kato, M.; Kamigaito, M.; Sawamoto, M. *Macromolecules* **1996**, *29*, 6979. (e) Percec, V.; Barboiu, B. *Polym. Prepr. (Am. Chem. Soc., Div. Polym. Chem.)* **1997**, *38*, 733. (f) Haddleton, D. M.; Jasieczek, C. B.; Hannon, M. J.; Shooter, A. J. *Macromolecules* **1997**, *30*, 2190. (g) Grimaud, T.; Matyjaszewski, K. *Macromolecules* **1997**, *30*, 2216. (h) Nishikawa, T.; Ando, T.; Kamigaito, M.; Sawamoto, M. *Macromolecules* **1997**, *30*, 2244. (i) Uegaki, H.; Kotani, Y.; Kamigaito, M.; Sawamoto, M. *Macromolecules* **1997**, *30*, 2249.
- (42) (a) Sigwalt, P. *Makromol. Chem., Macromol. Symp. Ed.* **1991**, *47*, 179. (b) Matyjaszewski, K. *J. Polym. Sci., Polym. Chem. Ed.* **1993**, *31*, 995. (c) Matyjaszewski, K. *Macromolecules* **1993**, *26*, 1787.
- (43) Shibaev, V. P.; Kostromin, S. G.; Plate, N. A. *Eur. Polym. J.* **1982**, *18*, 651.
- (44) Percec, V.; Hahn, B. *Macromolecules* **1989**, *22*, 1588.
- (45) Wang, Y.; Pugh, C., work in progress. Since chain-transfer constants are per repeat unit of the polymer, we are measuring chain transfer to polymer ($C_p = k_{tr,p}/k_p$) for a variety of SCLCPs using the Mayo equation and standard kinetic measurements of chain-transfer constants to a transfer agent that corresponds to one repeat unit of the polymer.
- (46) March, J. *Advanced Organic Chemistry*, 3rd ed.; Wiley-Interscience: New York, 1985; p 23.
- (47) Heintz, A. M.; Pugh, C., unpublished results.
- (48) Fredrickson, G. H.; Liu, A. J.; Bates, F. S. *Macromolecules* **1994**, *27*, 2503.
- (49) See for example, Vemulapalli, G. K. *Physical Chemistry*, 3rd ed.; Prentice Hall: Englewood Cliffs, NJ, 1993; Chapter 9.3.
- (50) Noirez, L.; Keller, P.; Cotton, J. P. *Liq. Cryst.* **1995**, *18*, 129.
- (51) Flory, P. J. *Macromolecules* **1978**, *11*, 1138.

MA971279F